**İSTANBUL TECHNICAL UNIVERSITY ★ INSTITUTE OF SCIENCE AND TECHNOLOGY**

# INVESTIGATION OF BAKE HARDENING PROPERTIES OF STEEL SHEETS

**M.Sc. Thesis by**

**Seval TÜRKOĞLU, B.Sc.**

**Department :** **Metallurgical and Materials Engineering**

**Programme:** **Materials Engineering**

**FEBRUARY 2006**

**İSTANBUL TECHNICAL UNIVERSITY ★ INSTITUTE OF SCIENCE AND TECHNOLOGY**

# INVESTIGATION OF BAKE HARDENING PROPERTIES OF STEEL SHEETS

**M.Sc. Thesis by**

**Seval TÜRKOĞLU, B.Sc.**

**(506021115)**

**Date of submission : 02 March 2006**

**Date of defence examination: 01 February 2006**

**Supervisor (Chairman): Prof. Dr. E. Sabri KAYALI**

**Members of the Examining Committee Prof.Dr. E. Sabri KAYALI (İTÜ.)**

**Prof.Dr. Hüseyin ÇİMENOĞLU (İTÜ.)**

**Prof.Dr. Mehmet KOZ (MÜ.)**

**JFEBRUARY 2006**

## FOREWORD

I am profoundly grateful to my thesis advisor, Prof. E. Sabri KAYALI, for his guidance throughout my graduate study. I should to thank to Prof. H.Çimenoğlu for his elaborate critics, suggestions on my experimental work and for his patience. I also thank all Mechanic Group research assistances in İTU. Finally I dedicate this work to my family, İhsan, Nursel, Sanlı TÜRKOĞLU and Emrah F. ÖZDOĞRU for their unconditional love and unlimited patience.

**February, 2006** **Seval TÜRKOĞLU**

## CONTENT

**ABBREVIATIONS** ..... **iv**
**LIST OF TABLES** ..... **v**
**LIST OF FIGURES** ..... **vi**
**LIST OF SYMBOLS** ..... **x**
**ÖZET** ..... **xi**
**SUMMARY** ..... **xii**

**1. INTRODUCTION** ..... **1**

**2. AUTOMOTIVE SHEET STEELS** ..... **5**
2.1. High strength Low Alloy (HSLA) Steel ..... 6
2.2. Interstitial Free (IF) Steels ..... 8
2.3. Dual Phase (DP) Steels ..... 9
2.4. Transformation Induced Plasticity (TRIP) Steels ..... 11
2.5. Bake Hardenable (BH) Steels ..... 14

**3. BAKE HARDENING** ..... **15**
3.1. Mechanism of Bake Hardening ..... 15
3.1.1. Cottrell Effect ..... 16
3.1.1.1. Strain Aging ..... 16
3.1.1.2. Interstitial Atoms ..... 17
3.2. The Measuring Method for Bake Hardenability ..... 18
3.3. Parameters Affecting The Bake Hardening ..... 20
3.3.1. Chemical Composition ..... 20
3.3.1.1. Influence of solute carbon and nitrogen content ..... 20
3.3.1.2. The Influence of Nitride and Carbide Former Elements ..... 22
3.3.1.3. Role of Sulfur and Manganese on BH- effect ..... 23
3.3.2. Production Parameters ..... 24
3.3.1.1. Temperature of Slab Heating ..... 24
3.3.1.2. Annealing temperature and Holding Time ..... 25
3.3.1.3. Cooling rate and Temperature ..... 28

**4. EXPERIMENTAL STUDY** ..... **29**

**5. RESULTS AND DISCUSSION** ..... **31**
5.1. Characteristic of the Examined Steels ..... 31
5.2. Strain Aging Behavior of the Steel ..... 33
5.3. Bake Hardening Behavior of the Steel ..... 38

**6. CONCLUSION** ..... **43**

**REFERENCES** ..... **44**

**APPENDIX** ..... **47**

**BIOGRAPHY** ..... **65**

## ABBREVIATIONS

| | |
|---|---|
| **AHSS** | **:** Advanced High Strength Steel |
| **DP** | **:** Dual Phase |
| **TRIP** | **:** Transformation Induced Plasticity |
| **IF** | **:** Interstitial Free |
| **HSLA** | **:** High Strength Low Alloy |
| **BH** | **:** Bake Hardenable |
| **TMCP** | **:** Thermo mechanical Controlled Processing |
| **YS** | **:** Yield Strength |
| **TS** | **:** Tensile strength |
| **WH** | **:** Work hardening |
| **TEM** | **:** Transmission Electron Microscope |
| **CA** | **:** Continuous Annealing |
| **ULC** | **:** Ultra Low Carbon Steels |
| **BCC** | **:** Body Centered Cubic |
| $\mathbf{T_{rh}}$ | : Slab Reheat Temperature |

**TABLE LIST**


| | | **Page Number** |
|---|---|---|
| **Table 1.1.** | **:**Summary of North American Target properties for 2005 for high strength light gage sheet steels for specific passenger cars ……..... | **2** |
| **Table 2.1.** | **:**Chemical compositions of given HSLA steels grades, wt. %. | **7** |
| **Table 2.2.** | **:**Mechanical properties of given HSLA steels grades……... | **7** |
| **Table 2.3.** | **:**Chemical compositions of given IF steels grades..... | **8** |
| **Table 2.4.** | **:**Typical chemical composition of a dual-phase steel, wt. %.... | **9** |
| **Table 2.5.** | **:**Typical mechanical properties of dual-phase steels…… | **9** |
| **Table 2.6.** | **:**Typical chemical composition of TRIP steels. wt. %..... | **12** |
| **Table 2.7.** | **:**Mechanical properties of TRIP450/800 steel grade…… | **12** |
| **Table 2.8.** | **:**The mechanical properties of different BH steel grades…….. | **14** |
| **Table 4.1.** | **:**Chemical composition of the experimental steels, ppm……..... | **30** |
| **Table 5.1.** | **:**Mechanical properties of as-received samples…… | **33** |
| **Table 5.2.** | **:**Aging time correspond to the maximum hardness value on "Normalized Hardness – Aging Time" graphs……. | **36** |
| **Table 5.3.** | **:**The calculated activation energies of strain aging for the examined steels……..…….. | **37** |
| **Table 5.4.** | **:**The activation energies of carbon and nitrogen diffusion in BCC iron…….. | **37** |
| **Table 5.5.** | **:**BH-effect corresponding to various pre-strain ratios and aging time at 170$^{o}$C……. | **40** |
| **Table B.1.** | **:**The results of hardness measurements conducted on the samples after aging for steel A…… | **51** |
| **Table B.2.** | **:**The results of hardness measurements conducted on the samples after aging for steel B…… | **52** |
| **Table B.3.** | **:**The results of hardness measurements conducted on the samples after aging for steel C……. | **53** |

**Table B.4.** **:**The results of hardness measurements conducted on the samples after aging for steel D…… **54**

**FIGURE LIST**

**Page Number**


**Figure 1.1. :** Applications of bake hardenable sheets used in automobile, bonnets (a), front fender (b), quarter panels (c), door panels (d)…….. **3**

**Figure 2.1. :** Relationship between yield strength and total elongation for various types of automobile sheet steels…… **5**

**Figure 2.2. :** Relationship between ultimate tensile strength and total elongation for various types of automobile sheet steels…… **6**

**Figure 2.3. :** Thermomechanical Controlled Processing of HSLA Steel…… **7**

**Figure 2.4. :** Schematic microstructure of DP steel…..... **10**

**Figure 2.5. :** Comparing the quasi-static stress-strain behavior of high strength, low-alloy (HSLA) steel to a DP steel of similar yield strength……..... **10**

**Figure 2.6. :** Processing schema of Dual-Phase and TRIP sheet steels…….. **11**

**Figure 2.7. :** A schematic TRIP steel microstructure……..... **12**

**Figure 2.8. :** Comparing the quasi-static stress-strain behavior of HSLA 350/450, DP 350/600 and TRIP 350/450 steels……... **13**

**Figure 2.9. :** Comparison of work hardening (WH) and bake hardening (BH) for TRIP, DP, and HSLA steels…….. **14**

**Figure 3.1. :** The mechanism of the BH effect……. **16**

**Figure 3.2. :** The mechanism for strain age hardening and the measuring method for bake hardenability (BH) in a tensile test…… **19**

**Figure 3.3. :** BH-effect as function of solute carbon…… **21**

**Figure 3.4. :** BH-effect as function of Nb/C……. **23**

**Figure 3.5. :** Dependence of the content of free carbon [C] (*a*) and the BH effect (*b*) on the annealing temperature of steels alloyed with Ti and possessing various Nb_C ratios after coiling at 770°C [27] □)Nb/C=0.52; Δ)Nb/C=0,57; ◊)Nb/C=0,78, o) Nb/C= 0,94; X) Nb/C = 1,35…….. **25**

**Figure 3.6. :** Solute carbon as function of annealing temperature (steel Nb/C = 0,74 is Ti free)…….. **26**

**Figure 3.7. :** Yield strength as a function of annealing temperature cold-rolled steels (tc= 770$^{o}$C) with various Nb/C ratios □) 0.5; Δ ) 0,6; ◊)0.8; o)0,9; x)1,3…….. **27**

**Figure 3.8. :** Effect of annealing time on BH for N1 steel (annealed at 880$^{o}$C and water quenched)…….. **27**

**Figure 3.9. :** Effect of cooling rate on $\Delta\sigma_{BH}$ for N1 steel (annealed at 890$^{o}$C for 1minute)……. **28**

**Figure 5.1. :** Stress – strain curves of as-received steels…… **32**

**Figure 5.2. :** Micro structures of saples used in experimental studies..... **33**

**Figure 5.3. :** Normalized hardness values for different aging time at 145$^{o}$C

(a), 170°C (b), 200°C (c), and 220°C (d)…….. **35**
**Figure 5.4.** **:**The precipitation start temperature of the compounds for Ti/Nb stabilized steels……. **38**
**Figure 5.5.** **:**BH-effect of steel A (a), steel B (b), steel C (c), and steel D (d) for pre-strain level 2%,5%,10% at 170°C……. **41**
**Figure 5.6.** **:**BH-effect of 2% pre-strain (a), 5% pre-strain for steel (b), 10% pre-strain (c) for steel A, B, C and D at 170°C……. **43**
**Figure A.1** **:**Microstructure of Steel A, as-recieved. (X500)…….. **47**
**Figure A.2** **:**Microstructure of Steel A, as-recieved. (X1600)…… **47**
**Figure A.3** **:**Microstructure of Steel B, as-recieved. (X500)…….. **48**
**Figure A.4** **:**Microstructure of Steel B, as-recieved. (X1600)…… **48**
**Figure A.5** **:**Microstructure of Steel C, as-recieved (X500)……... **49**
**Figure A.6** **:**Microstructure of Steel C, as-recieved (X1600)……. **49**
**Figure A.7** **:**Microstructure of Steel D, as-recieved (X1600)……. **50**
**Figure C.1** **:**ln (1/tr) vs. (1/T) graphs for steel A…… **55**
**Figure C.2** **:**ln (1/tr) vs. (1/T) graphs for steel B…… **55**
**Figure C.3** **:**ln (1/tr) vs. (1/T) graphs for steel D…… **56**
**Figure D.1** **:**Stres-Strain curve of 2%, 5% and 10% predeformed Steel A at 10, 15, 20, 30 minute aged sample, a) 2% predeformed-10min. aged, b)2% predeformed 15min. aged, c)2% predeformed 20min. aged, d)2%predeformed 30min. aged, e) 5% predeformed 10min. aged, f)5% predeformed 15min. aged, g)5% predeformed 20min. aged, h)5%predeformed 30min. aged, i) 10% predeformed 10min. aged, j)10% predeformed 15min. aged, k)10% predeformed 20min. aged, l)10%predeformed30min.aged……. **58**
**Figure D.2** **:**Stres-Strain curve of 2%, 5% and 10% predeformed Steel B at 10, 15, 20, 30 minute aged sample, a) 2% predeformed-10min. aged, b)2% predeformed 15min. aged, c)2% predeformed 20min. aged, d)2%predeformed 30min. aged, e) 5% predeformed 10min. aged, f)5% predeformed 15min. aged, g)5% predeformed 20min. aged, h)5%predeformed 30min. aged, i)10% predeformed 10min. aged, j)10% predeformed 15min. aged, k)10% predeformed 20min. aged,……... **60**
**Figure D.3** **:**Stres-Strain curve of 2%, 5% and 10% predeformed Steel C at 10, 15, 20, 30 minute aged sample, a) 2% predeformed-10min. aged, b)2% predeformed 15min. aged, c)2% predeformed 20min. aged, d)2%predeformed 30min. aged, e) 5% predeformed 10min. aged, f)5% predeformed 15min. aged, g)5% predeformed 20min. aged, h)5%predeformed 30min. aged, i)10% predeformed 10min. aged, j)10% predeformed 15min. aged, k)10% predeformed 20min. aged, l)10%predeformed30min.aged……. **62**
**Figure D.4** **:**Stres-Strain curve of 2%, 5% and 10% predeformed Steel D at 10, 15, 20, 30 minute aged sample, a) 2% predeformed-10min. aged, b)2% predeformed 15min. aged, c)2% predeformed 20min. aged, d)2%predeformed 30min. aged, e) 5% predeformed 10min. aged, f)5% predeformed 15min. aged, g)5% predeformed 20min. aged, h)5%predeformed 30min. aged, i)10% predeformed 10min. aged,j) 10% preformed 15 **64**

min.aged, k)10% preformed 20 min.aged……...

## LIST OF SYMBOLS

| | |
|---|---|
| $\sigma$ | : Stress |
| **R** | : Gas constant |
| **T** | : Absolute aging temperature |
| $t_r$ | : Time to reach max hardness |
| $A_r$ | : Pre-exponential constant |
| $Q_r$ | : Activation energy of strain aging |
| $r_m$ | : Coefficient of normal plastic anisotropy |

## ÇELİK SACLARIN FIRINDA SERTLEŞME ÖZELLİĞİNİN İNCELENMESİ

## ÖZET

Otomotive endüstrisinin önemli bir amacı şekillendirilebilirlik ve mukavemet özellikleri korunarak otomobil ağırlığından tasarruf sağlamaktır. Fırında sertleşebilen çeliklerin geliştirilmesi, hem şekillendirilebilirlik hem de mukavemet gereklerini yerine getirerek bu soruna etkili bir çözüm olmuştur. Şekillendirilen parçalar boyandıktan sonra boyayı kurutma amacıyla 170 $^{o}$C ve 20 dk fırınlanır. Bu işlem esnasında akma mukavemetinde görülen artış, fırında sertleştirme olarak tanımlanır. Fırınlama sertleşmesi ile akma mukavemetinde $\Delta\sigma 0,2$ = ~ 30 -60 MPa arasında artış olur. Boya pişirme işlemi sırasında akma mukavemetinde görülen artış deformasyon yaşlanması mekanizması ile açıklanır. Fırında sertleşmeye sebep olan ferrit içinde çözünmüş olan C ve N atomlarıdır.

Bu çalışmada kullanılan dört farklı kalite çelik ERDEMİR A.Ş'den temin edilmiştir. Çeliklerin orijinal haldeki karakterizasyonu, mikroyapı çalışması, çekme testi ve sertlik ölçümleri ile yapılmıştır. Deformasyon yaşlanması davranışı sertlik ölçümü ile ve fırında sertleşme davranışı çekme testi ile incelenmiştir. Yapılan sertlik ölçümleri sonucunda BH-etkisinin sertlik değerlerindeki değişim ile belirlenebileceği anlaşılmıştır. Ve deformasyon sertleşmesi davranışının kinetik incelemesi yapılmıştır. Elde edilen aktivasyon enerjisi değerleri karbon ve azotun HMK demir içindeki yayınma aktivasyon enerjisi değerlerine uygunluk göstermiştir. Maksimum BH-etkisi %2'lik ön deformasyon ile elde edilmiştir. Deformasyon yaşlanması kinetikleri karbonun yayınması ile açıklanan A ve B kalite çeliklerde maksimum BH değerlerine yaşlanma işleminin 20. dakikasında ulaşılırken deformasyon yaşlanması kinetiği azotun yayınması ile açıklanan D kalite çelikte 10. dakikada ulaşılmıştır.

**INVESTIGATION OF BAKE HARDENING PROPERTIES OF STEEL SHEETS**


## SUMMARY

The main objective of automotive industry is decreasing the weight of body car panels while maintaining good formability and mechanical properties. The development of bake hardenable steels offers an interesting solution which can satisfy both the formability and strength requirements. After press-forming, the panels go to paint-baking cycle, at 170$^{o}$C for 20 minutes. During the paint-baking cycle, an increase in yield strength occurs, which is referred to as bake hardening. Bake hardening can produce a 30 – 60 MPa increase in strength after press forming. The strength increase during the paint baking process is a consequence of strain aging and is controlled primarily by the amount of interstitial carbon or nitrogen in the ferrite matrix.

In this study, four different steel grades supplied from ERDEMİR. Characterization of the steels as-received conditions was carried out by microstructral examinations, tensile tests and hardness measurements. We investigated the strain aging behavior of the steels by hardness measurements, and the bake hardening behaviors by tensile test. Hardness measurements showed that BH effect can be examined by the change in hardness. So, we investigate the kinetics of age hardening by using hardness values. The calculated activation energies for the examined steel grades were in good agreement with the activation energy of carbon or nitrogen diffusion in BCC iron. The maximum BH-effect was obtained at the level of 2%. Maximum hardness values was reached at the 20$^{th}$ min of aging for steel A and steel B which are related to the C atoms diffusions to the dislocations and 10$^{th}$ min for Steel D that the strain aging kinetic explained by N atoms diffusion.

# 1. INTRODUCTION

Two important objectives being pursued by the automobile industry are a decrease in car weight and improvements in safety [1]. The threat of future legislation regarding fuel consumption has forced the automotive industry to develop lighter, more fuel efficiency vehicles. Accessories such as air bags, impact protection, electric windows and air conditioning add considerable weight to the car and this must be balanced by a reduction in weight of the automobile exposed panels [2] which will lower the volume of exhausted $CO_2$ gas and the fuel consumption. Consequently, reduction of body weight, which accounts for approximately 25% of total vehicle weight, has become an important technical issue [3]. On the other hand, automobile panels press formed from sheet steel have become larger and complicated. This integration of press formed parts demands higher press formability than that of conventional sheet steels [4]. To realize these requirements, reduction in sheet thickness, higher strength, and improvements in press formability are generally demanded for automobile body panels. Target properties to be met by automotive steels in 2005 are given in Table 1.1. The use of higher strength steels allows thinner gauge components and reduces the total weight. However, conventional high strength sheet steels have in sufficient formability to meet the drawing requirements of today's more complex outer-body car panels. Bake hardenable high strength steels are an interesting solution that can satisfy all these requirements. Bake-hardenable steel is any steel that exhibits a capacity for a significant increase in strength through the combination of work hardening during part formation and strain aging during a subsequent thermal cycle, such as a paint-baking operation [5]. Increasing of yield strength in bake-hardening steels is due to an artificial aging process within the already manufactured sheet. It is caused by the blocking of initially mobile dislocations when free carbon atoms diffuse toward the dislo

cations, forming Cottrell atmospheres or iron-carbide precipitates. Usually this effect takes place during the baking operation after painting at 170°C for 20 minutes [6]. These steels have excellent formability during press forming and an increased strength in the end product due to bake hardening resulting from paint baking that is carried out on the finished components [7]. This property provides a capacity for a strength increase of approximately 30 to 60 MPa from the initial yield strength [8]. Since it requires no additional processes, the bake hardening does not significantly affect production costs, and it may also allow a greater final strength level to be achieved in higher formability grades.

**Table1.1** Summary of North American Target properties for 2005 for high strength light gage sheet steels for specific passenger cars [2].

| **Application** | **Thickness mm** | **Tensile strength MPa** | **Yield strength MPa** | **Total Elongation %** |
|---|---|---|---|---|
| **Doors, outer skin** | 0.66 | 363 | 237 | 36 |
| **Doors, inner structure** | 0.64 | 335 | 201 | 40 |
| **Hood, outer skin** | 0.66 | 359 | 244 | 36 |
| **Hood, internal structure** | 0.64 | 345 | 197 | 38 |
| **Trunk lid outer skin** | 0.66 | 362 | 238 | 36 |
| **Trunk lid internal structure** | 0.64 | 345 | 205 | 39 |
| **Fenders, quarter panels** | 0.66 | 348 | 221 | 39 |
| **Floor pan** | 0.75 | 362 | 200 | 39 |
| **Internal body stucture** | 0.9 | 414 | 285 | 35 |
| **Roof** | 0.67 | 372 | 233 | 36 |

Bake-Hardening steel is increasingly used by the automobile industry for the outer panels of cars [6]. These parts widens the range of application of such steels to door panels, bonnets and tops ,doors, deck lids, quarter panels, fenders, hoods, and roofs as illustrated in figure 1.1[9- 13]. The components mentioned above results a weight saving of of ~ 7 kg per car [2].

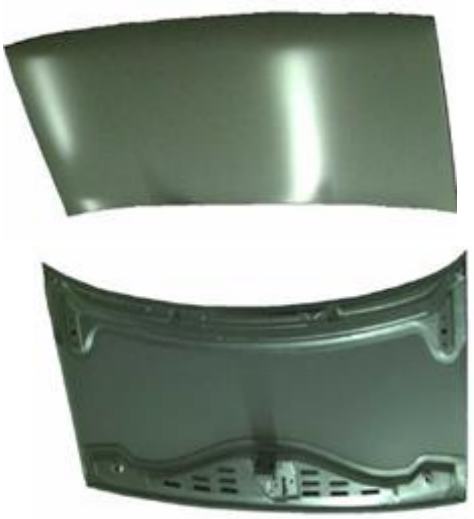

(a)

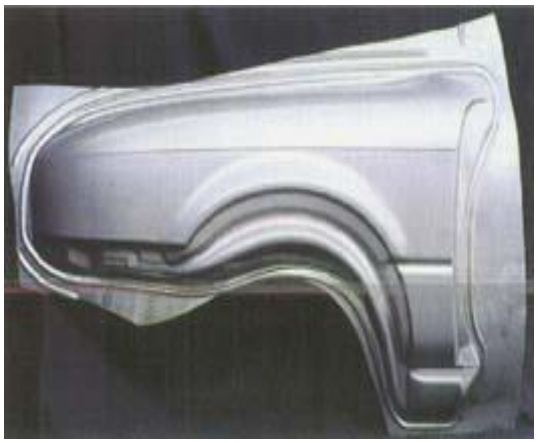

(b)

(c)

(d)

**Figure 1.1.** Applications of bake hardenable sheets used in automobile, bonnets (a), front fender (b), quarter panels (c), door panels (d) [10- 13].

In the present study hardness measurements and tensile tests of steel sheets has been carried out to find out the strain aging and the bake hardening behaviors of the steel sheets supplied from ERDEMİR, respectively.

## 2. AUTOMOBILE SHEET STEELS

A large range of strength levels are available for the sheet steels utilized in automobile. Figure 2.1 and figure 2.2 show the general relationship between yield strength-tensile strength and total elongation for automobile sheet steels which can be classified as; Advanced High Strength Steel (AHSS) which include Dual Phase (DP) and transformation induced plasticity (TRIP) steels. Interstitial Free (IF) steels, High Strength Low Alloy (HSLA) steels and Bake Hardenable (BH) steels

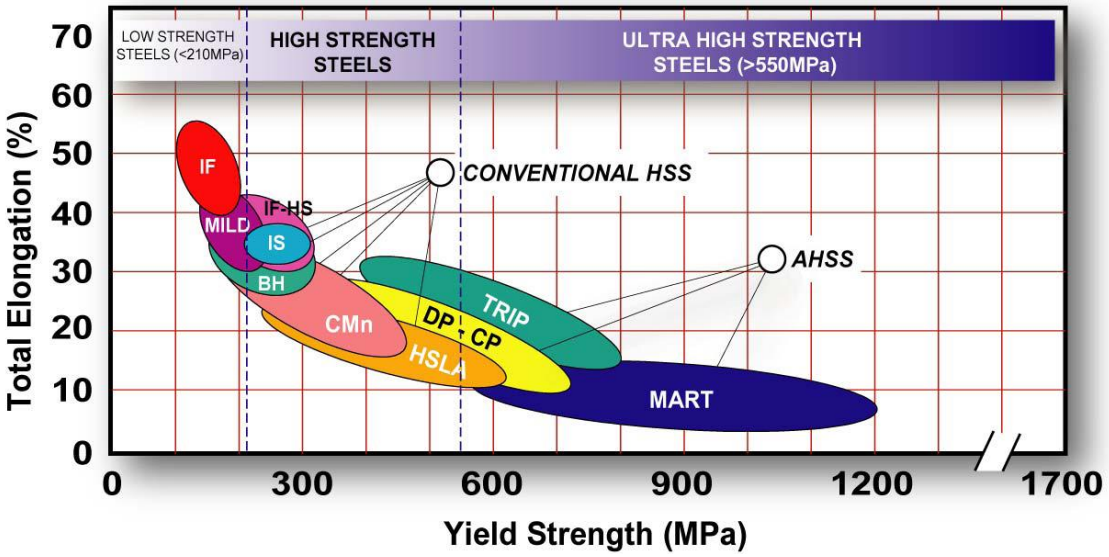


**Figure 2.1.** Relationship between yield strength and total elongation for various types of automobile sheet steels [14].

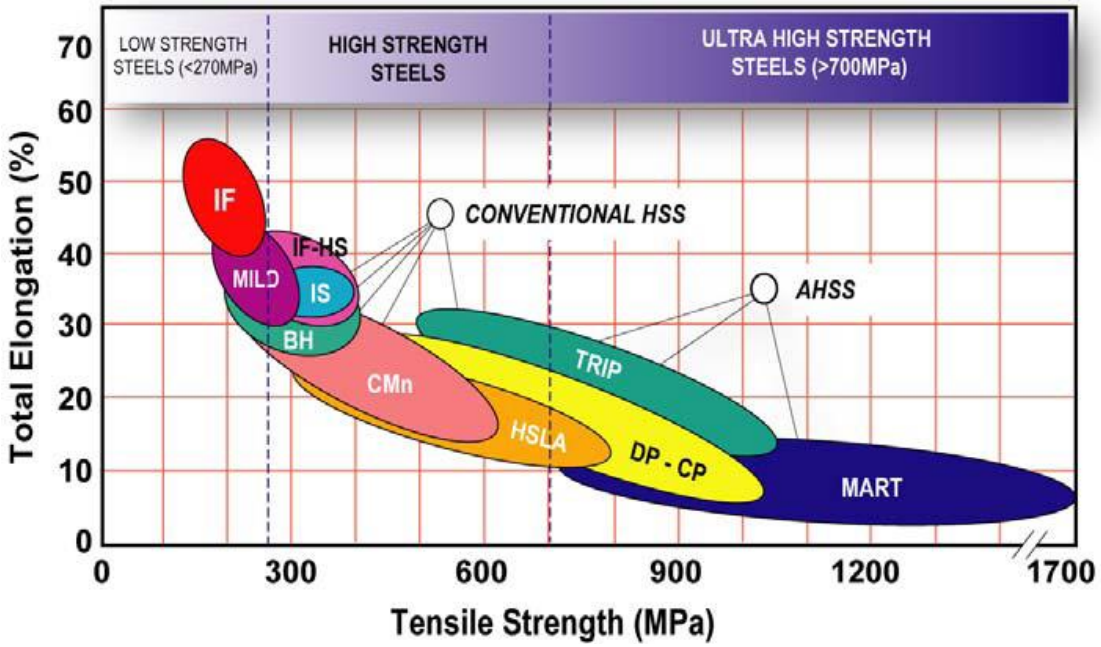


**Figure 2.2.** Relationship between ultimate tensile strength and total elongation for various types of automobile sheet steels [14].

### 2.1. High Strength Low Alloy (HSLA) Steels

High strength low alloy steel (HSLA) grades have a good combination of formability and weldability. Compared to conventional carbon steels. HSLA Steels have: Higher strength, Better toughness; Better formability/drawability; Better weldability; and Better corrosion resistance. The strength of HSLA steels is achieved by the addition of small quantities of alloying elements. The main purpose of HSLA steel processing is to produce the fine and homogeneous ferrite grains as well as a high volume fraction of carbide/nitride precipitates during or after austenite-ferrite transformation. This process results in superior mechanical properties such as high strength, toughness, and good ductility and weldability. These purposes can be achieved by Thermomechanical Controlled Processing (TMCP) as schematically described in the figure 2.3 below [15].

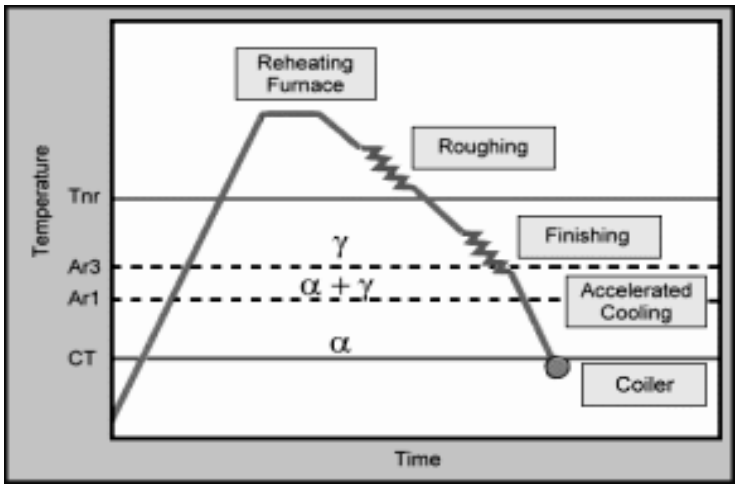


**Figure 2.3.** Thermomechanical Controlled Processing of HSLA Steel [15].

Chemical compositions and mechanical properties of HSLA steels are presented in table 2.1 and table 2.2, respectively.

**Table 2.1.** Chemical compositions of given HSLA steels grades, wt. % [15].

| **Grade JIS** | **C Max (%)** | **Mn Max (%)** | **P Max (%)** | **S Max (%)** | **Si Max (%)** | **Nb Max (%)** | **V Max (%)** | **Ti Max (%)** |
|---|---|---|---|---|---|---|---|---|
| G 3113 | 0.18 | 1.2 | 0.02 | 0.006 | 0.05 | - | - | 0.02 |
| G 3134 | 0.17 | 1.5 | 0.02 | 0.006 | 0.05 | 0.025 | - | 0.02 |

**Table 2.2.** Mechanical properties of given HSLA steels grades [15].

| **Grade JIS** | **Yield Strength (MPa)** | **Tensile Strength (MPa)** | **Elongation (%)** |
|---|---|---|---|
| G 3113 | 360 - 440 | 480 - 570 | 38 - 44 |
| G 3134 | 410 - 520 | 580 - 690 | 30 - 36 |

## 2.2. Interstitial Free (IF) steels

Interstitial Free (IF) steel was firstly introduced in Japan in the 70's. Nowadays, IF Steel has world widely known as the best affordable high quality material for deep drawing applications. Automotive applications ranging from panel hood, panel roof, panel door, to fuel tank. IF Steel was developed after extensive research and practices of improving the performance of traditional low carbon steel. By a combination of very low carbon content (< 80 ppm) and an addition of titanium or niobium microalloying elements, IF Steel theoretically does not have any interstitial atoms such as carbon, hydrogen, oxygen, nitrogen, at the crystal lattice [16]. This combination results in an extraordinary formability as well as a non-aging property. IF Steel is made by a special production route which starts from steelmaking into hot rolling and cold rolling processes that is significantly different from the route of an ordinary low carbon steel quality. Hot liquid steel is decarburized in 10mbar depressed RH- vacuum vessel, so that carbon content decreases from 400 ppm into 20 ppm. After killing of the liquid steel by addition of aluminum ingot, titanium or niobium alloys are added. The cast slabs are continuously rolled at high rolling temperature (above A3 line) to achieve uniform and large austenite grains. The hot strip must be cooled at higher coiling temperature to fully precipitate TiN or NbC particles. The process parameters as well as the chemistry of steel are also unlike the other steel products. The table 2.3 below shows a few of IF steel typical chemistry.

**Table 2.3**. Chemical compositions of given IF steels grades.

| **IF Steel Type** | **Weight (%)** | | | | | | | |
|---|---|---|---|---|---|---|---|---|
| | **C** | **Si** | **Mn** | **P** | **S** | **N** | **Ti** | **Nb** |
| Ti alloyed type | 0.0030 | 0.015 | 0.20 | 0.015 | 0.02 | 0.0025 | 0.045 | --- |
| Nb alloyed type | 0.0020 | 0.020 | 0.20 | 0.015 | 0.02 | 0.0030 | --- | 0.040 |
| Ti-Nb alloyed | 0.0035 | 0.030 | 0.20 | 0.015 | 0.02 | 0.0040 | 0.015 | 0.060 |

## 2.3. Dual Phase (DP) Steel

Dual phase steels are a new class of high-strength low alloy steels. The term dual phase refers to predominance in the microstructure of two phases, ferrite and martensite. However, small amounts of other phases, such as bainite, pearlite or retained austenite, may also be present [17, 18]. Figure 2.4 shows the processing schema of Dual-Phase and TRIP sheet steels. Dual-phase steels have a microstructure with 80 to 90% polygonal ferrite and 10 to 20% martensite islands dispersed throughout the ferrite matrix. In general, dual phase steels have a carbon content of less then %0.1. The carbon content also produces about 20% of the martensite in the microstructure after intercritical annealing and rapid cooling [16]. Typical chemical composition and mechanical properties of DP450 steel are given in table 2.4 and table 2.5, respectively.

**Table 2.4.** Typical chemical composition of a dual-phase steel, wt. %.

| | %C | %Si | %Mn | %P | %S | %Cr |
|---|---|---|---|---|---|---|
| DP450 | 0,036 | 0,043 | 1,22 | 0,018 | 0,006 | 0,66 |

**Table 2.5.** Typical mechanical properties of dual-phase steels.

| Steel Grade | Yield Strength (MPa) | Tensile Strength (MPa) | Elongation% |
|---|---|---|---|
| DP450 | 450 | 750 | 18 |

Figure 2.4 shows a schematic microstructure of DP steel, which contains ferrite plus islands of martensite. The soft ferrite phase gives these steels excellent ductility. When these steels deform, strain is concentrated in the lower-strength ferrite phase surrounding the islands of martensite, creating the unique high work-hardening rate exhibited by these steels. The work hardening rate plus excellent elongation give DP steels much higher ultimate tensile strengths than conventional steels of similar yield strength.

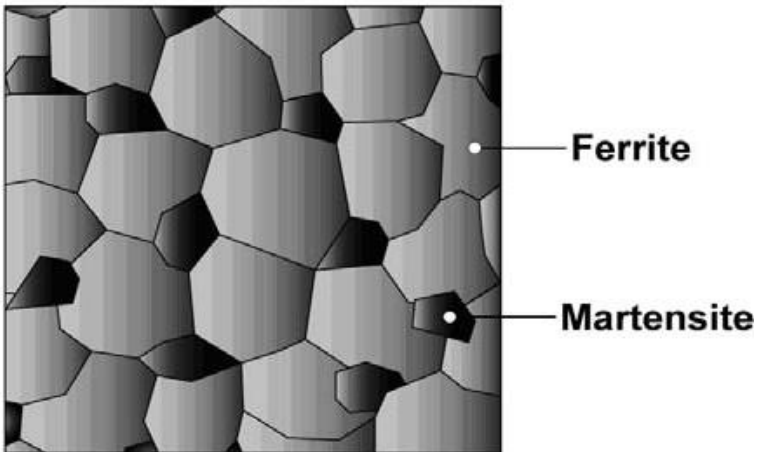


**Figure 2.4.** Schematic microstructure of DP steel [14].

Figure 2.5 compares the quasi-static stress-strain behavior of high-strength, low-alloy (HSLA) steel to a DP steel of similar yield strength. The DP steel exhibits higher initial work hardening rate, higher ultimate tensile strength, and lower YS/TS ratio than the similar yield strength HSLA. DP steels and other Advanced High Strength Steels (AHSS) also have a bake hardening effect that is an important benefit compared to conventional steels.

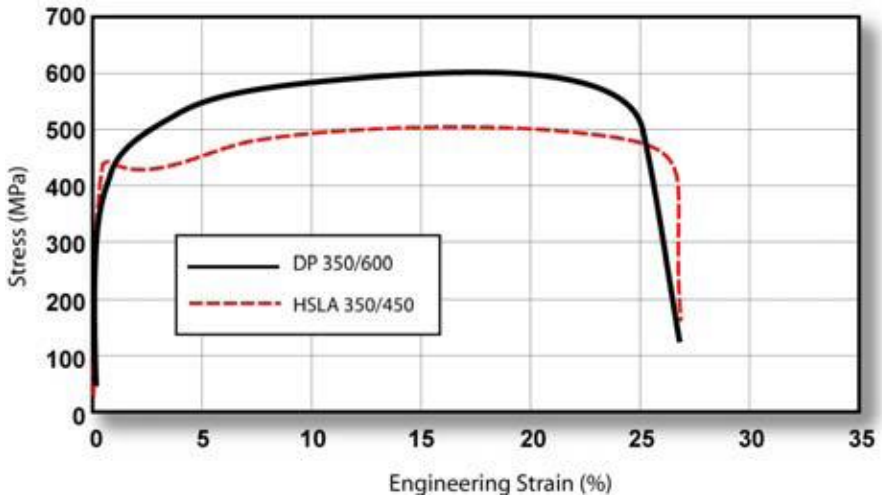


**Figure 2.5.** Comparing the quasi-static stress-strain behavior of high-strength, low-alloy (HSLA) steel to a DP steel of similar yield strength [14].

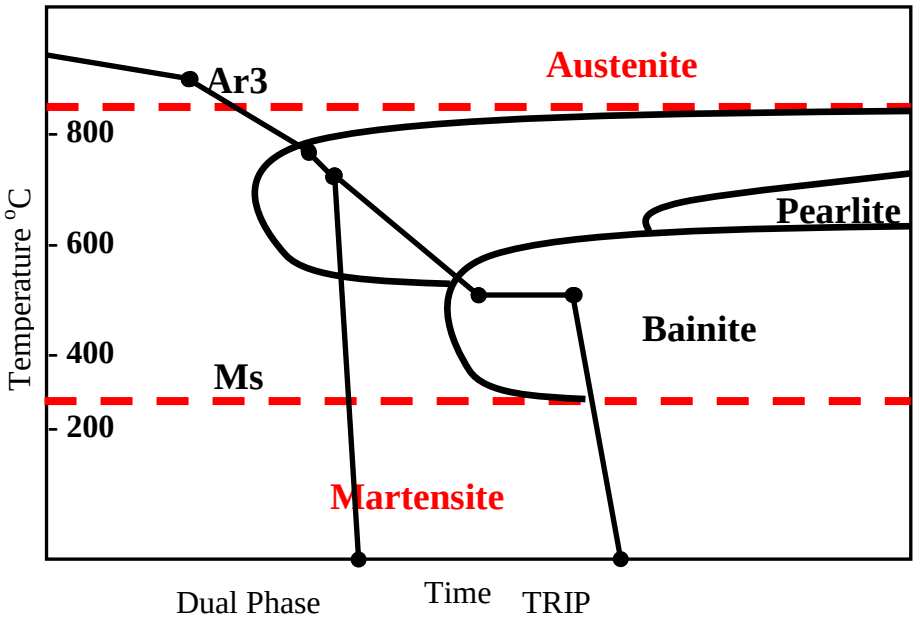


**Figure 2.6**. Processing schema of Dual-Phase and TRIP sheet steels [19].

If the steel is rapidly cooled from the intercritical annealing temperature (figure 2.6.), then the austenite undergoes a martensitic transformation, resulting in a so-called ‘’dual-phase’’ steel consisting of ferrite plus martensite, usually with small amounts of retained austenite, if cooling is arrested and transformation is accomplished at an intermediate temperature, then microstructure consisting of bainitic ferrite with larger quantities of austenite can also be obtained after final cooling to room temperature.

### 2.4. Transformation Induced Plasticity (TRIP) Steels

Transformation Induced Plasticity steel (TRIP) is steel with a microstructure of retained austenite embedded in a primary matrix of ferrite. In addition to a minimum of 5 volume percent of retained austenite, hard phases such as martensite and bainite are present in varying amounts. Typical chemical composition and mechanical properties of TRIP 450/800 steel grade are given in table 2.6. and table 2.7., respectively. The main phenomenon responsible for the improved mechanical properties has been proposed to be the deformation-induced transformation of the metastable retained austenite to martensite during straining [20]. A schematic TRIP steel microstructure is shown in figure 2.7. The strain level at which retained austenite begins to transform to martensite can be designed by adjusting the carbon content. At lower carbon levels, the retained austenite begins to transform almost

immediately upon deformation, increasing the work hardening rate and formability during the stamping process. At higher carbon contents, the retained austenite is more stable and begins to transform only at strain levels beyond those produced during forming. At these carbon levels the retained austenite persists into the final part. It transforms to martensite during subsequent deformation, such as a crash event. TRIP steels can therefore be engineered or tailored to provide excellent formability for manufacturing complex AHSS parts or to exhibit high work hardening during crash deformation to provide excellent crash energy absorption. The morphology of the retained austenite is also important for the stabilization. The best elongation behavior has been observed when the retained austenite is present as films between the subunits of bainite, rather than as blocky regions between sheaves of bainitic ferrite [21].

**Table 2.6**. Typical chemical composition of TRIP steels. wt. %.

| Steel Grade | %C | %Si | %Mn | %P | %S | %Al | %Fe |
|---|---|---|---|---|---|---|---|
| TRIP450/800 | 0,170 | 1,04 | 1,33 | 0,006 | 0,006 | -------- | Bal. |

**Table 2.7**. Mechanical properties of TRIP450/800 steel grade.

| Steel Grade | Yield Strength(MPa) | Tensile Strength (MPa) | Elongation% |
|---|---|---|---|
| TRIP450/800 | 450 | 800 | 26-32 |

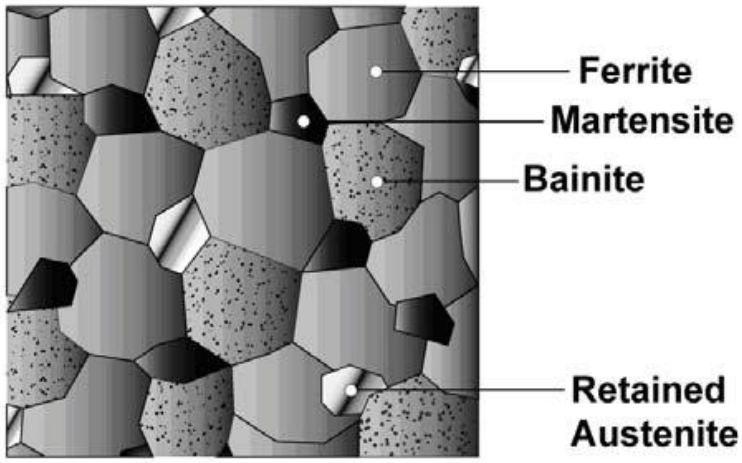


**Figure 2.7**. A schematic TRIP steel microstructure [14].

The stress-strain behavior of HSLA, DP and TRIP steels of approximately similar yield strengths are compared in figure 2.8. The work hardening rates of TRIP steels are substantially higher than for conventional HSS, providing significant stretch forming and unique cup drawing advantages. This is particularly useful when designers take advantage of the high work hardening rate (and increased bake hardening effect) to design a part utilizing the as-formed mechanical properties. The high work hardening rate persists to higher strains in TRIP steels, providing a slight advantage over DP in the most severe stretch forming applications.

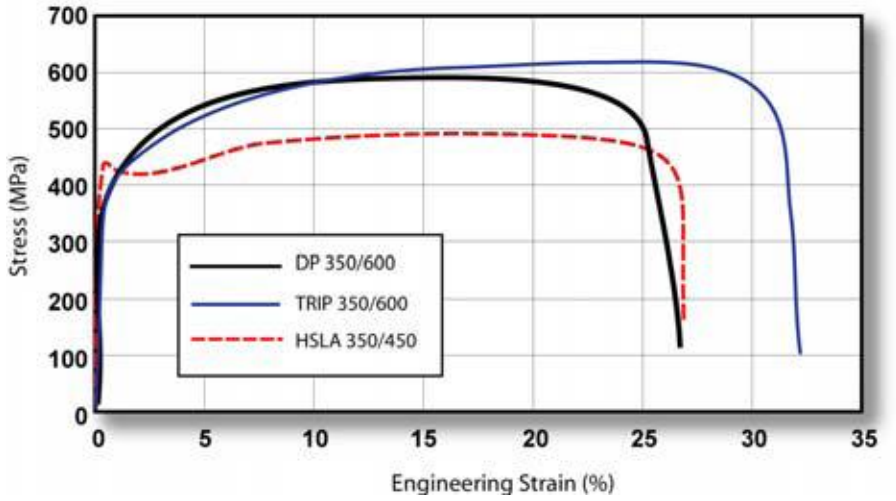


**Figure 2.8.** Comparing the quasi-static stress-strain behavior of HSLA 350/450, DP 350/600 and TRIP 350/450 steels.

Figure 2.9 shows the work hardening and bake hardening increases for the pre-strained and baked tensile specimen. The HSLA shows little or no bake hardening, while AHSS such as DP and TRIP steels shows large positive bake hardening index. The DP steel also has significantly higher work hardening than HSLA or TRIP steel because of higher strain hardening at low strains.

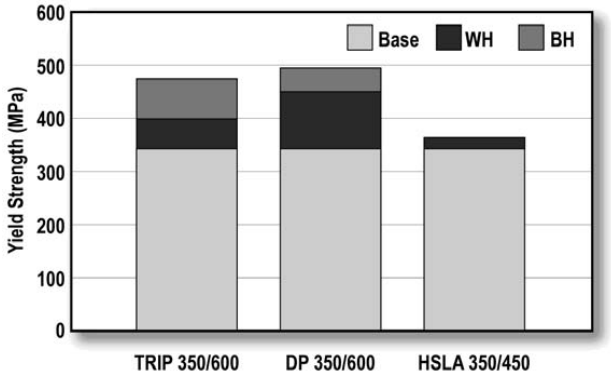


**Figure 2.9.** Comparison of work hardening (WH) and bake hardening (BH) for TRIP, DP, and HSLA steels [14].

### 2.5. Bake Hardenable (BH) Steels

A bake-hardenable steel is any steel that exhibits a capacity for a significant increase in strength through the combination of work hardening during part formation and strain aging during a subsequent thermal cycle, such as a paint-baking operation [13].

The carbon atoms in the steel sheet are kept in the solid-solution condition. This can be accomplished by rapid cooling of the steel sheet from high temperature during the sheet production process, and this rapid cooling has become industrially possible by the development of the continuous annealing technique for strips. Before the development of the continuous annealing technique, rapid cooling was impossible because annealing of heavy coil with big heat capacity was conducted as a batch process.

A combination of relatively low yield strength prior to manufacturing and high in-part strength after forming and paint baking makes bake-hardenable steels ideal for applications where dent and palm printing resistance is important. These steels are made in the following grades as illustrated in Table 2.8.

**Table 2.8.** The mechanical properties of different BH steel grades, [13].

| Steel Grade | Yield Strength [MPa] | Tensile Strength [MPa] | Elongation [%] |
|---|---|---|---|
| BH180 | 196 | 325 | 38.9 |
| BH210 | 196 | 325 | 38.9 |
| BH240 | 196 | 325 | 38.9 |

## 3. BAKE HARDENING

### 3.1. Mechanism of Bake Hardening

The bake hardening effect corresponds to the ability for the metal to harden during the paint baking process [22].

Sheet steel containing a small amount of solute carbon exhibits low yield strength as-received before press-forming. After press-forming by plastic deformation, the induced dislocations result in work hardening of the sheet steel. Car bodies are bake painted after press forming and assembling, the press formed parts being heated at approximately 170°C during the bake painting process. After this process, the dislocations induced by press forming are stabilized by solute carbon diffusing adjacent to the core of a dislocation. A higher stress is required to promote the slip movement that occurs with plastic deformation of the stabilized dislocations when an external stress is applied to press formed and bake-painted parts. Thus, a bake hardenable sheet steel exhibits a low yield strength before press forming ,and a high yield strength in a completed car after bake painting [4].

Bake hardening is essentially a strain aging process involving interactions between interstitial atoms and dislocations. It results in an increase in yield strength**.**

To realize this strength increase, the following criteria must be met:

(i) Mobile dislocations must be present in the steel.

(ii) There must be sufficient concentration of solute in the steel top in these dislocations.

(iii) The solute must be mobile at the aging temperature

(iv) Dislocation recovery must be sufficiently slow to prevent softening [23].

Current theory proposes that the increase in yield strength during paint baking occurs by a two step pr

ocess: step one is the segregation of carbon to pin dislocations by the Cottrell effect and step two, the strengthening by precipitations of fine carbides. First step generally completed before the second step begins. The mechanism of the BH effect is schematically presented in Figure 3.1.

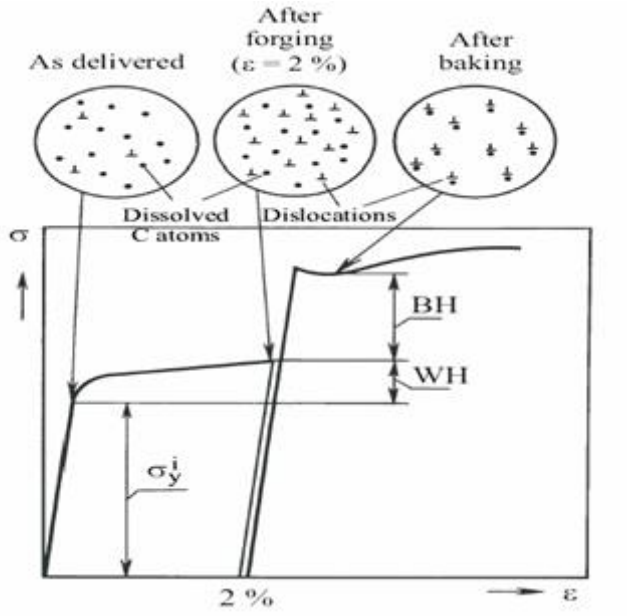


**Figure 3.1**. The mechanism of the BH effect [9]

### 3.1.1. Cottrell Effect

During the paint baking cycle, the first step is initiated by the segregation of carbon atoms to dislocations. Cottrell atmospheres then form, which effectively anchor the dislocations. The carbon atoms produce tetragonal distortions as well as dilation. The former interacts with screw dislocations and the latter with edge dislocations, given rise to increase in strength [24]. This is a form of static strain aging.

#### 3.1.1.1. Strain Aging

Strain aging is a type of behavior, usually associated with the yield-point phenomenon, in which the strength of a metal is increased and the ductility is decreased on heating at a relatively low temperature after cold-working [17]. This occurs by the interaction, during or after plastic deformation, of point defects and dislocations. When they occur during plastic deformation, the process is termed dynamic strain aging. When the property changes occur after plastic deformation, the process is termed static strain aging.

Strain aging can be a valuable and economical means of strengthening steels. The most common measure of property changes during strain aging is the effects produced on the load – elongation curves in a uniaxial tensile test.

Strain aging can be divided into two stages. Initially, there is a small rise in yield strength, which is completed within the first seconds of aging in the stress field of a dislocation. This is known as the Snoek-effect i.e. the stress induced ordering of interstitial atoms in the lattice under an applied stress. Because of the very small time intervals involved in this process, it is not easily measured and has largely been ignored [25]. The second and slower stage is caused by long range diffusion of the interstitial solute atoms towards the dislocations core. These atoms concentrate in the stress field of a dislocation and form a Cottrell atmosphere. The incurred interaction energy between the solute and the dislocation's strain field anchor the dislocations effectively and gives rise to the increase in strength. Once all mobile dislocations are saturated with carbon atoms, further segregation will lead to the formation of clusters and fine carbide precipitates as a third stage. The carbon in solution remained constant, indicating that dislocation locking was no longer dominant. The formation of coherent $\varepsilon$ carbide on dislocations is the mechanism most likely to explain this third stage. Previous investigations [26] in which a second strength increase was seen attempted to confirm the presence of such carbides using TEM. No particles were observed, and it was concluded that, if they do exist, they are too small to be viewed by this method [25]. The structure or morphology of these carbides has not yet been determined. However, from experiments performed by [27] it is believed that the carbides form coherent particles in the matrix. The yield strength obtained after straining and aging is hence dependent on the local dislocation density and the solute concentration. These parameters are influenced by: the amount of strain and the work hardening rate of the steel during the pre-straining, the initial level and location of dissolved interstitial atoms, and the ferrite grain size [6].

#### 3.1.1.2. Interstitial Atoms

It is expected that the magnitude of strain aging will be proportional to the concentration of interstitial solute atoms in the matrix. The size of the upper yield point is controlled by the formation of Cottrell atmospheres that lock the dislocations during aging. It has been found that the quantity needed to completely lock

dislocations is quite small. A nitrogen content of 1 ppm can produce a detectable change in the mechanical properties of steel and 10 to 20 ppm can completely lock all dislocations.

Nitrogen plays a more important role in the strain aging of iron than carbon because it has higher solubility and diffusion coefficient and produces less complete precipitation during slow cooling [17]. Interstitial carbon and nitrogen atoms are very mobile in ferrite iron at ambient temperatures. The temperatures less than 100°C, the solubility of nitrogen is approximately 100 times greater than that of carbon [28].

To control strain aging, it is usually desirable to lower the amount of carbon and nitrogen in solution by adding elements which will take part of the interstitials out of solution by forming stable carbides or nitrides. Aluminum, vanadium, titanium, columbium, and boron have been added for this purpose. While a certain amount of control over strain aging can be achieved, there is no commercial low-carbon steel which is completely non-strain aging. It is important to eliminate strain aging in deep-drawing steel because the reappearance of the yield point can lead to difficulties with surface markings or 'stretcher strains' due to the localized heterogeneous deformation [17].

### 3.2. The Measuring Method for Bake Hardenability

The BH effect is evaluated by tensile test with a standard procedure. The Tensile Test Specimens of annealed and planished steel are deformed with degree $\sigma = 2\%$ and deformed tensile specimen aged for 20 min at 170°C. Following this step, tensile test is carried out at room temperature.

BH effect $\Delta\sigma$ Mpa obtain by the difference between yield point of prestrained specimen with degree $\sigma = 2\%$ and lower yield point of aged specimen.

Figure 3.2 represents the mechanism for strain age hardening and the measuring method for bake hardenability (BH) in a tensile test.

The procedure employed to assess the BH is the following;

(1) the specimen strained 2 % pct at room temperature
(2) the sample is aged at $170^{o}$C for 20 minutes, and
(3) the specimen is tensile tested at room temperature

The amount of bake hardening is determined by subtracting the flow stress after the 2 pct. prestain from the lower yield strength after baking. Although a 2 pct. prestrain and aging at 170$^{o}$C for 20 minutes are typical values employed to cause bake hardening in steels.

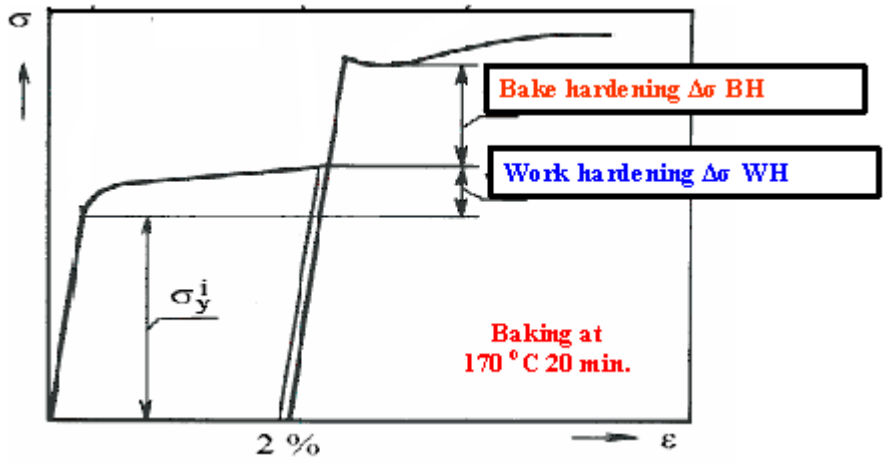


**Figure 3.2.** The mechanism for strain age hardening and the measuring method for bake hardenability (BH) in a tensile test.

### 3.3 Parameters Affecting the Bake Hardening

#### 3.3.1. Chemical Composition

##### 3.3.1.1. Influence of solute carbon and nitrogen content

The strength increase in modern bake hardening steel depends primarily on interstitial solute atoms. The interstitial solute atoms like carbon and nitrogen have a pinning effect on dislocations during deformation [29]. To improve sheet formability, major attention has been focused on reducing the total amount of carbon and nitrogen during steelmaking and the removal of these interstitial elements from solid solution by the addition of stabilizing alloying additions. The content of nitrogen in the steel should be at a level of 20 – 50 ppm. Nitrogen is usually considered to be effectively removed from solid solution by the formation of AlN or TiN precipitates at high temperatures, which is required for preventing aging at room temperature. Nitrogen has a faster diffusion rate at room temperature than carbon ($1.34 \times 10^{16}$ $cm^2s^{-1}$ and $2.8 \times 10^{17}$ $cm^2s^{-1}$) which allows it to diffuse through the ferrite matrix and pin dislocations during the storage of the steel at ambient temperatures. The slower diffusion rate of carbon allows the steel to remain at storage temperatures up to six months without aging. Bake hardenable steels must contain a certain minimum amount of solute carbon. This interstitial element is responsible for the strength increment as bake hardening occurs by static strain aging as a result of interstitial atom segregation to dislocation. In the initial stages of strain aging, the strengthening is accomplished solely by the formation of solute atmospheres. Increasing the carbon content will increase the bake hardening response: more solute is available to pin mobile dislocations and the formation of clusters will occur more rapidly. Van Snick *et al* [30] Showed that increasing the carbon content from 0 to 40 ppm increased the bake hardening response from 40 to 70 MPa: further increase in solute carbon had no effect on the bake hardening measured, On the other hand, excessive amounts of carbon in solution lead to room temperature aging [2]. Increased amount of solute C easily diffuses in steel, even at ambient temperature. Consequently, bake hardening sheet steels containing solute C might suffer from a deterioration of mechanical properties due to aging before pres-forming by vehicle producers. Decreasing the solute carbon concentration in steels usually produces excellent formability [29].

These limitations help the researcher to find out excellent steels in order to have sufficient susceptibility for bake hardening. The amount of free carbon needed for the desired BH effect is evaluated differently by different researchers. By the data of [2] ferrite should contain 15 – 25 ppm free carbon for a BH effect of 30 – 60 MPa. By the data of [5, 6] for a BH effect of 40 MPa it is sufficient that the amount of free carbon in ferrite be about 6 ppm. Figure 3.3 a-b shows the BH effect as a function of solute carbon, respectively. The possibility of the BH effect without natural aging of the steel is limited to about 60 MPa.

Rubianes and Zimmer categorized the effect of increasing carbon content on bake hardening and room temperature aging into tree domains. At<3ppm solute carbon steel have excellent room temperature stability but show no significant bake hardening. The second domain consists of steels containing>7 ppm solute carbon. The bake hardening response is excellent exceeding 60 MPa. Unfortunately, the propensity for room temperature aging is also greatly increased in these steels. The third domain applies to steel with carbon contents which have an adequate bake hardening response of 20 – 60 MPa but also offer suitable resistance to room temperature aging. Obviously bake hardening steels should be designed to fall in this region. Independently of the type of the steel a BH effect of 40 MPa is virtually guaranteed when the carbon content in the solid solution is equal or greater than 6 ppm [10].

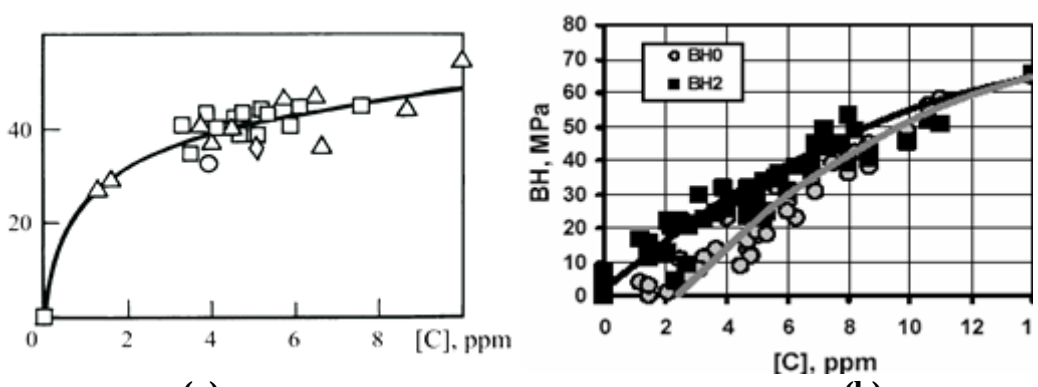


**Figure 3.3**. BH-effect as function of solute carbon, [10,32]

### 3.3.1.2 The Influence of Nitride and Carbide Former Elements

To control the amount of interstitial elements such as C and N in solid solution, micro alloying elements play an important role. Some of these are titanium, niobium and vanadium. We can represent the role of primary microalloying elements as follows.

***Titanium:*** Titanium is an important element added to increase strength and hardness of steel by grain-size control (grain refinement). It is very strong carbide and nitride former and also a strong deoxidizer [32].

During steel making with addition of Ti, reactions progress as follows. Ti binds nitrogen and TiN nitride, binds carbon and sulfur into carbosulfide $Ti_4C_2S_2$, and forms TiC titanium carbide. Titanium carbonitride is a particle with the initial dissolution temperature exceeding 950°C (which is much higher than the temperature of annealing of cold-rolled steel). Therefore, the carbon bound in the carbosulfide cannot contribute to the BH effect. In this connection, in the case of the use of steels alloyed with Ti and Nb the content of titanium should be limited to a level required only for full binding of nitrogen. Microalloying with titanium alone can cause difficulties connected with the formation of carbonitride (inevitable loss of a certain amount of carbon) [9].

***Niobium:*** Niobium binds carbon into NbC carbides, and forms segregations on the boundaries of ferrite grains. The presence of niobium in the solid solution and on grain boundaries improves the texture of the steel. The authors of [6] assume that microalloying with niobium alone is favorable for the production of steels with hot zinc bearing coatings. Nitrogen is stabilized in such steels by using aluminum; they contain aluminum nitrides and bear no niobium nitrides. The authors of [6] also mention that the content of dissolved carbon in steels with niobium is higher than in titanium-bearing steels. Figure 3.4 shows the BH-effect as function of Nb/C.

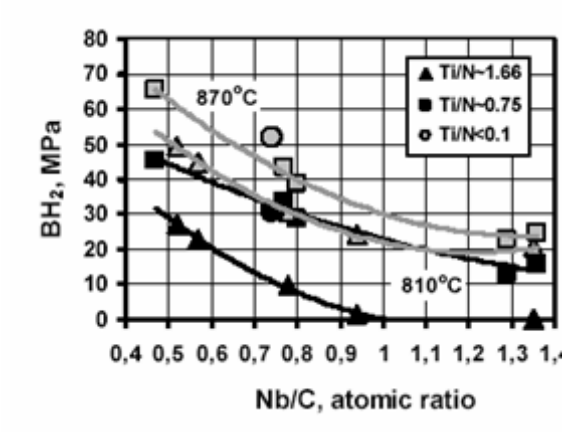


**Figure 3.4.** BH-effect as function of Nb/C, [32]

***Vanadium**:* Vanadium is an important element added to increase strength and hardness of steel by grain-size control (grain refinement) as well as to increase hardenability. It is a strong nitride former; also forms a carbide and minimizes loss in strength during tempering, [32].

VC carbides dissolve well at a relatively low temperature, and vanadium-alloyed steels are highly resistant to natural aging and poorly sensitive to changes in the process parameters. Some recent works [33] describe vanadium-alloyed steels with a BH effect. However, it should be noted that steels with vanadium are now in the stage of laboratory development and require further investigation.

### 3.3.1.3 Role of Sulfur and Manganese on BH- effect

***Sulfur (S)*** is usually considered an impurity added to special steels for improved machinability. [32]

The results of the studies performed in [34] show the importance of the presence of sulfur for the formation of BH effect. The BH effect can be increased by decreasing the content of sulfur because it suppresses the segregation of the TiS sulfide and the growth of the amount of the $Ti_4C_2S_2$ carbosulfide insoluble under conventional annealing temperatures. The increase in the sulfur content from 10, 30 to 80 ppm causes a marked reduction of the BH effect. However, the effect of sulfur is ambiguous and depends on the content of other elements, primarily carbon and titanium. Comparison of the results obtained shows that the increase in the content of sulfur decreases the BH effect in steels of type *II* (with a high concentration of titanium) but increases it in steels of type *I* (with a low concentration of titanium) [9].

***Manganese (Mn)*** is an essential alloying element added to increase solid-solution strength and hardness as well as to increase hardenability. It is weak carbide former and counteracts brittleness caused by sulfur (iron sulfide) through the formation of a manganese sulfide (MnS). High levels of manganese produce austenitic steel with improved wear and abrasion resistance [32].

The available data do not make it possible to describe the effect of manganese on the BH effect. Until recently, it was assumed that the increase in the content of manganese causes a decrease in the BH effect. This is validated by the fact that MnS manganese sulfides that segregate instead of TiS titanium sulfides serve as a substrate for the segregation of TiC thus removing carbon from the solid solution.

Thus, the influence of manganese on the BH effect in titanium- bearing steels is composite and depends on the proportion of the elements and the temperature to which the slab is heated. At a high heating temperature (1250°C) an increase in the content of manganese diminishes the BH effect because of the widened range of formation of titanium carbosulfide. On the contrary, at a low heating temperature of the slab (1050°C), growth in the manganese content intensifies the BH effect due to the appearance of an alternative to the formation of $Ti_4C_2S_2$ [9].

### 3.3.2 . Production Parameters

#### 3.3.2.1. Temperature of Slab Heating

Slabs are heated in slab heating furnace, temperatures ranges from 1000$^o$C to 1250$^o$C depending on the steels chemical composition and the dimension. Heating the slab to the reheat temperature ($T_{rh}$) influences the state of the precipitates, as well as providing the initial austenite grain size [35].

Optimum $T_{rh}$ will vary according to composition, because precipitate dissolution temperature varies according to the type and concentration of alloying elements. For example, in typical ULC steels, NbC is completely dissolved at 1000$^o$C, while $Ti_4C_2S_2$ and TiS do not dissolve at temperatures as high as 1250$^o$C. It has been indicated in the literature that a low $T_{rh}$ produces the best *r* and percent elongation values. This may be because the low $T_{rh}$ will allow carbon to remain stabilized in $Ti_4C_2S_2$ precipitates.

The content of Mn is also very important to determine the slab heating temperature. At a low content of manganese (up to 0.1%) the high temperature of slab heating (up to 1250°C) causes dissolution of titanium carbosulfide and formation of fine dispersed TiC titanium carbide particles (0.01 – 0.03 μm) that are relatively easily soluble in annealing, which leads to a BH effect. At a medium manganese content (0.15 – 0.20%), heating of the slab to 1250°C does not cause dissolution of the carbosulfide, as a result of which the BH effect can be low or even absent. At a high manganese content (0.5 – 1.5% and more) heating of the slab to 1000°C – 1050°C causes growth of manganese sulfide instead of titanium carbosulfide (changes the particle type), as a result of which carbon becomes free and the BH effect manifests itself. In addition, low-temperature heating of the slab improves the ductility and forgeability of ultralow carbon steels

### 3.3.2.2. Annealing temperature and Holding Time

The primary processes of the formation of the final structure (mechanical properties and the BH effect) and the solid solution is the stage of heat treatment of cold-rolled steel. In this connection, a correct choice of the annealing temperature is very important for obtaining an optimum combination of properties in the steel [36]. The carbon content in the solid solution of cold-rolled annealed steel increases with the annealing temperature figure 3.5. [37].

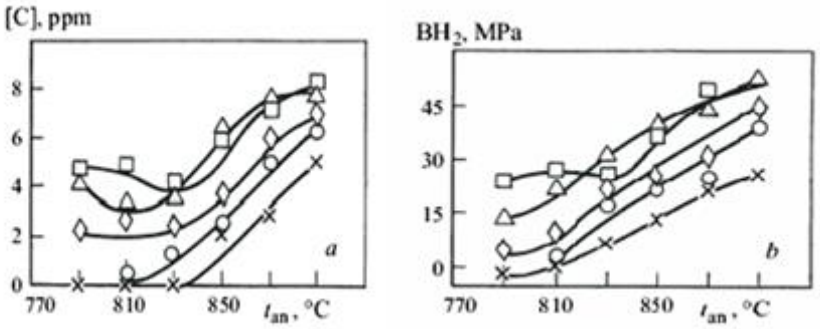


**Figure 3.5.** Dependence of the content of free carbon [C] (*a*) and the BH effect (*b*) on the annealing temperature of steels alloyed with Ti and possessing various Nb/C ratios after coiling at 770°C [27] □) Nb/C = 0.52, Δ ) Nb/C = 0,57

◊) Nb/C = 0,78 o) Nb/C= 0,94 X) Nb/C = 1,35 [8]

The solute carbon content increases continuously with higher annealing temperatures due to the dissolution of NbC. The effect of the annealing temperature on solute carbon content is shown by another example in figure 3.6.

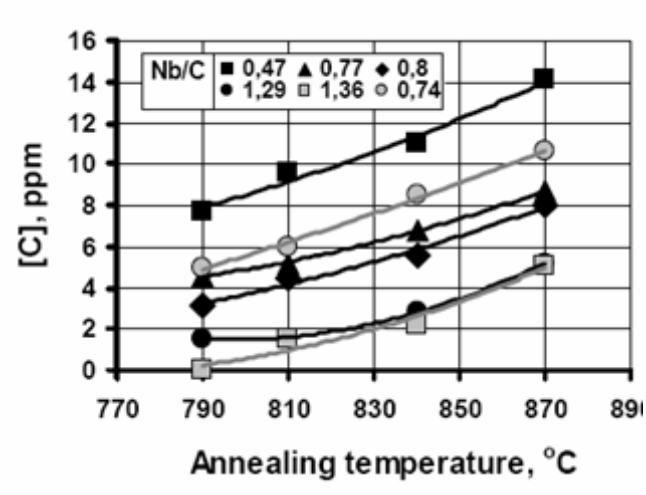


**Figure 3.6.** Solute carbon as function of annealing temperature (steel Nb/C = 0,74 is Ti free)

A high annealing temperature is favorable for good cold formability [31]. The mean coefficient of normal plastic anisotropy (*rm*) increases considerably with the increase in the annealing temperature.

The decrease in the yield strength observed with the growth in Nb/C is connected with the decrease in the content of dissolved carbon. However, at a higher annealing temperature a certain amount of NbC particles dissolves again, which weakens the effect of niobium as a carbonbonding element. This is well reflected in Figure 3.7 which presents the dependences of the yield strength on the annealing temperature.

For the steel with a hypo-stoichiometric composition (Nb/C = 0.5) the increase in the temperature is accompanied by a decline in the yield strength, whereas for the steel with a hyper stoichiometric composition (Nb/C =1.3) the yield strength grows [37].

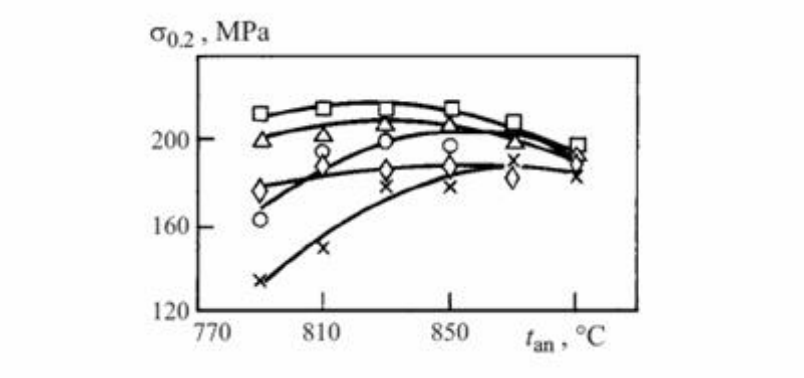


**Figure 3.7.** Yield strength as a function of annealing temperature cold-rolled steels (tc= 770$^{o}$C) with various Nb/C ratios □) 0.5; Δ ) 0,6; ◊)0.8; o)0,9; x)1,3 [8]

The extension of the hold time in annealing of steels within the actual process temperature range does not cause noticeable changes in the BH effect [38]. The variation in ΔσBH with annealing time for steel N1 held at 880$^{o}$C and then fast air cooled is shown in figure 3.8. ΔσBH increases to approximately 32 MPa in 3 minutes. After 3 minutes, no further change in the ΔσBH is seen. This suggested that the matrix has reached its solubility limit of carbon and/or niobium at 3 minutes. With no further increase in solute carbon, no further increase in bake hardening can occur. The high ΔσBH value of 27 MPa after 1 minute, compared to the maximum bake hardening value after 3 minutes, suggested that the majority of NbC dissolution occurs in the first minute of annealing.

Therefore, holding times greater than 1 minute don't significantly affect ΔσBH.

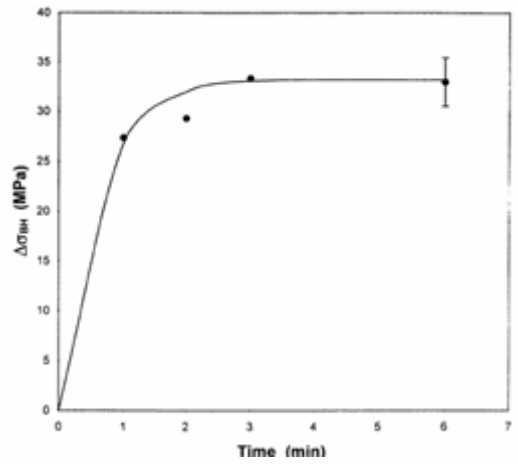


**Figure 3.8.** Effect of annealing time on BH for N1 steel (annealed at 880$^{o}$C and water quenched)

### 3.3.2.3. Cooling rate and Temperature

One of the methods to vary the solute carbon content in the steel is varying the cooling speed after soaking. The cooling rate after annealing influences the BH effect. This influence depends on the chemical composition of the steel. With the increase in the cooling rate of the steel with Nb/C ≡ 1.2 the BH effect intensifies. In the steel with Nb/C ≡ 0.25 the BH effect is virtually independent of the cooling rate [38]. An increase of the cooling rate leads to higher solute carbon content in the bulk of the grain. The variation in ΔσBH with cooling rate is shown in figure for N1 steel annealed at 890$^{o}$C for 1 minute. The three cooling rates: air, fast air, and water quench were used. ΔσBH decreases with decreasing cooling rate. With slower cooling rates, more dissolved carbon can return to the niobium clusters and /or iron and reprecipitate as NbC or $Fe_3C$ in their respective temperature ranges. Water quenching produces the least precipitation of NbC or $Fe_3C$ upon cooling and gives the highest value of $\Delta\sigma_{BH}$. figure 3.9 effect of annealing time on $\Delta\sigma_{BH}$ for N1 steel (annealed at 880$^{o}$C, wate quenched ). Slower cooling rates allow more time for re-precipitation, therefore resulting in less solute carbon [35].

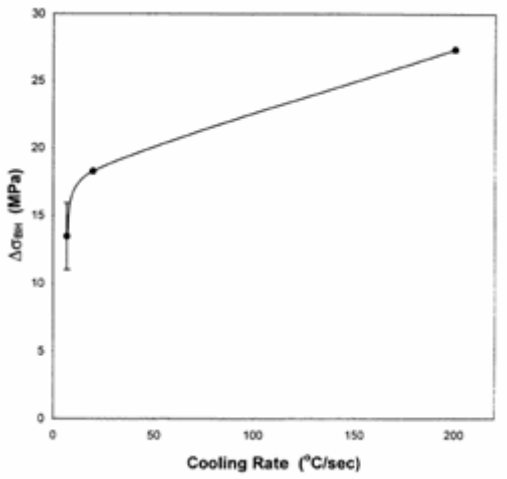


**Figure 3.9.** Effect of cooling rate on ΔσBH for N1 steel (annealed at 890$^{o}$C for 1 minute)

It is evident from the results that the variation in cooling rate after CA has a pronounced effect on the diffusion of carbon to the grain boundary, explaining bake hardening differences of the same material processed on different industrial lines.

Thus, a significant increase of the bake hardenability of the ULC bake hardening steels can be achieved through both a coarse grain size and a faster cooling [39].

## 4. EXPERIMENTAL STUDY

Strain aging and bake hardening behaviors of steels supplied from ERDEMIR was examined in this study. Chemical compositions of the examined steels are listed in Table 4.1. Characterization of the steels as-received conditions was carried out by microstructural examinations, tensile tests and hardness measurements.

Metallographic samples were grinded by 320 – 1200 mesh SiC abrasive papers and then polished by 1 μ diamond paste and final polishing was conducted on the fine grade $Al_2O_3$ slurry abrasive to achieve mirror like surface finish. After polishing, metallographic samples were etched with nital solution. Microstructures of the samples were examined by an optical microscope.

Hardness measurements were conducted on a Schimadzu HMV-2 microhardness tester under indentation load of 50 g by utilizing Vickers indenter. The hardness measurements performed after grinding with 320 and 1200 mesh SiC paper followed by polishing with fine grade $Al_2O_3$ slurry abrasive. The tensile tests were carried out by Dartec tensile test machine. Tensile test specimens were machined along the rolling direction of the sheets.

**Table 4.1.** Chemical composition of the experimental steels, ppm

| Steel Grade | Thicknes smm | C | Mn | S | Nb | Al | Ti | N | Nb*/C | Al*/N | Ti*/N |
|---|---|---|---|---|---|---|---|---|---|---|---|
| **A** | 0.7 | 34 | 4585 | 100 | 35 | 874 | 128 | 91 | -6.720 | 2.450 | -2.057 |
| **B** | 0.7 | 52 | 4815 | 65 | 186 | 940 | 206 | 72 | -4.250 | 3.472 | -0.558 |
| **C** | 0.8 | 38 | 1519 | 87 | 25 | 539 | 649 | 39 | -7.092 | 10.410 | 13.785 |
| **D** | 0.7 | 336 | 1489 | 87 | 13 | 414 | 17 | 57 | -7.690 | 4.578 | -3.121 |

This research is composed of two main parts;

- Investigation of the strain aging behavior of the steels by hardness measurements, and
- Investigation of the bake hardening behavior of the steels by tensile test.

Strain aging behavior of the steels were examined on samples (10mm x10mm) subjected to 2% tensile pre-strain. Specimens were aged at temperatures in between 145$^{o}$C and 220$^{o}$C in a Petrofer AS 135 salt bath, for various times and cooled in air. Hardness of the aged samples was measured after polishing the surfaces of the samples. Hardness measurements were made under indentation load of 50 g with a Vickers indenter. At least ten successive hardness measurements were averaged for each aging condition.

Hardness measurements performed for four different temperatures after pre-strained %2 showed that BH effect can be examined by the change in hardness values. At this point, new approach to investigate the kinetics of age hardening by using hardness values was included to our research.

General tendency for investigation of age hardening kinetic is using the yield strength values obtained by the tensile test. This needs various tensile test specimen and time. An easy method to achieve the same results is the hardness measurement. By this way researchers save both time and materials. For this research, Only 4 tensile specimens were sufficient for the kinetic observation which normally needs various specimens.

Bake hardenability of the steels were examined after applying 2%, 5% and 10% tensile pre-strains to the tensile test samples. Pre-strained tensile test specimens were then hold at 170$^{o}$C for various times in between 10 min and 30 min. after cooling to the room temperature, tensile test specimens were immediately subjected to tensile test.

## 5. RESULTS AND DISCUSSION

### 5.1. Characteristic of the Examined Steels

Stress – strain curves and microstructure of as-received steels are presented in figure 5.1.and Figure 5.2, respectively. Steel A and steel B have higher yield and tensile strength comparing to steel C and steel D. % elongations of steel A and steel B are at a level about 40%. Steel C and Steel D showed more elongation than that of Steel A and steel B. Transformation from elastic to plastic deformation is discontinuous for steel A and steel B while continuous for steel C and steel D. Table 5.1 illustrates the mechanical properties of as-received samples.

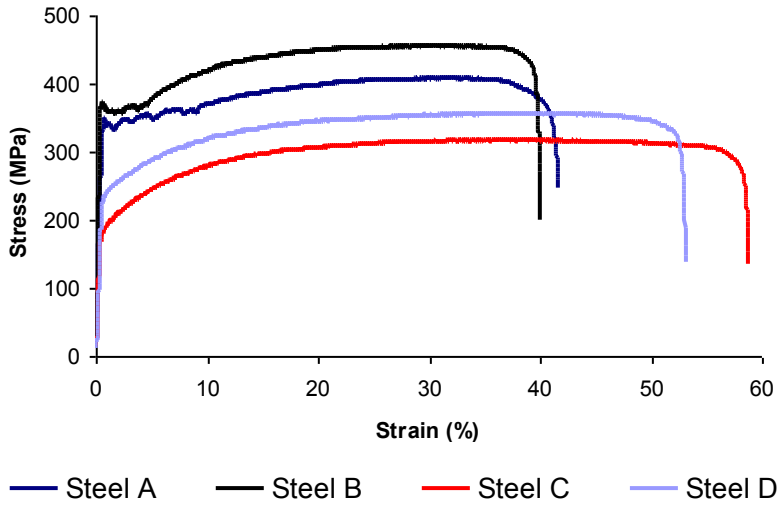


**Figure 5.1.** Stress – strain curves of as-received steels

**Table 5.1.** Mechanical properties of as-received samples

| Steel Grade | Yield Strength (MPa) | Tensile Strength (MPa) | Elongation % | Hardness (Vickers) |
|---|---|---|---|---|
| **A** | 340 | 403 | 41 | 160 |
| **B** | 358 | 455 | 40 | 165 |
| **C** | 180 | 315 | 58 | 120 |
| **D** | 228 | 355 | 53 | 135 |

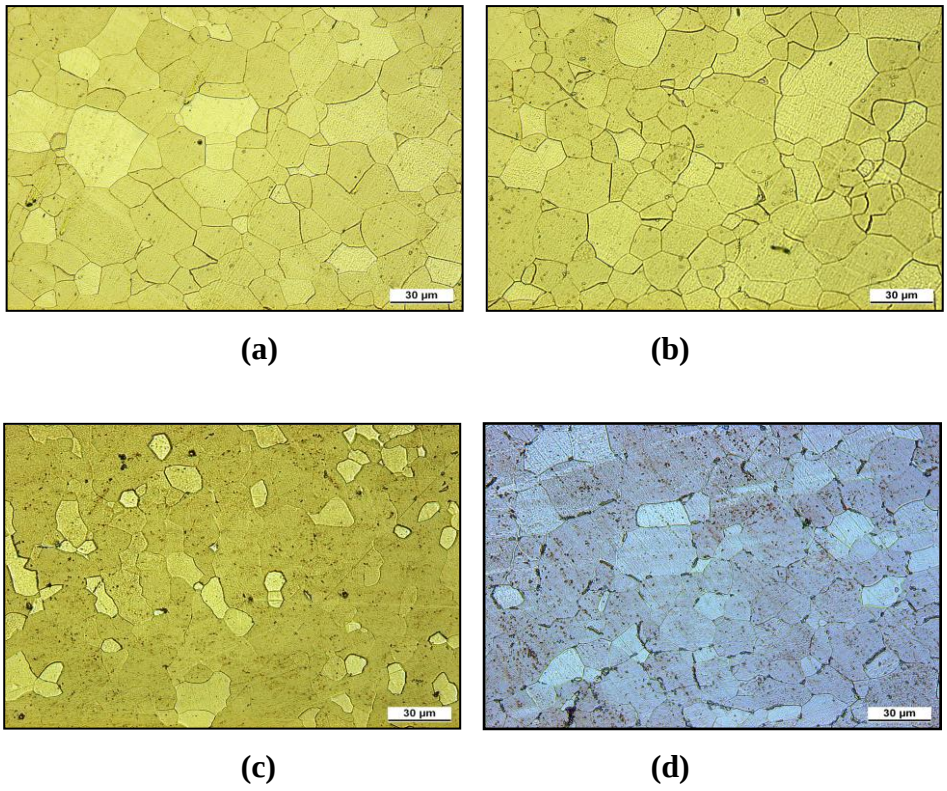


**Fig. 5.2.** Microstructure of Steel A (a), Steel B (b), Steel (c) and Steel D (d) as-received conditions (X800).

Some other microstructures of steel grades are listed in Appendix A.

### 5.2. Strain Aging Behavior of the Steel

The results of hardness measurements conducted on the samples after aging are listed in Appendix B Table 1-4. Normalized hardness was calculated by dividing the hardness at any time ($H_i$) to hardness of 2% pre-strained specimen ($H_o$) and multiplied by hundred and plotted in figure 5.3 as "Normalized Hardness – Aging Time" graphs.

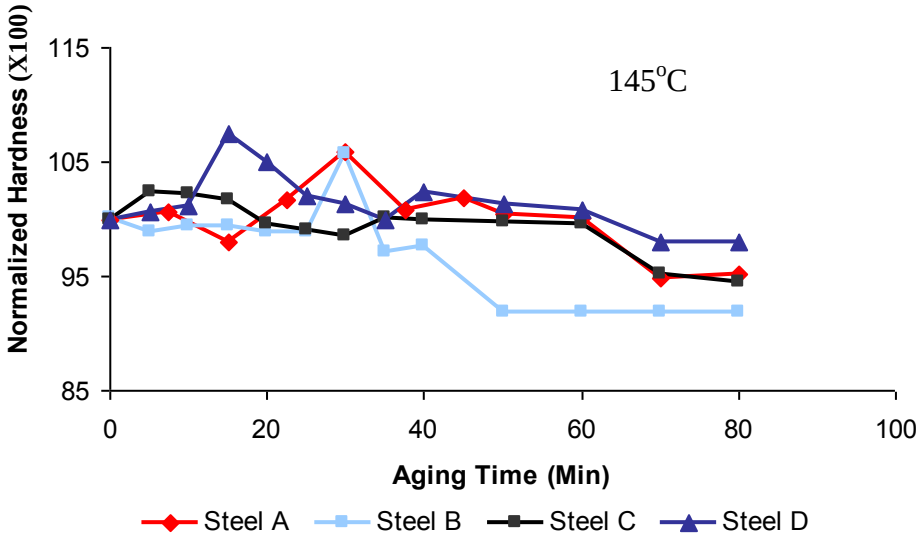


(a)

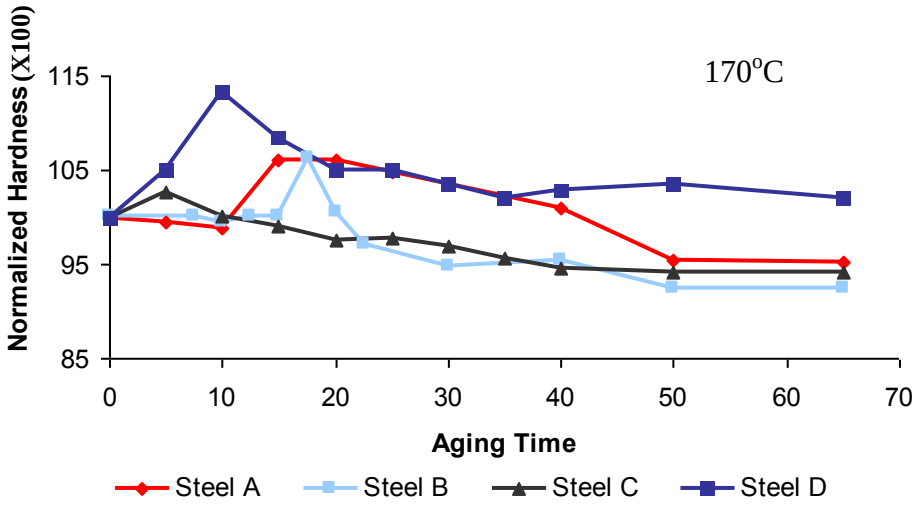

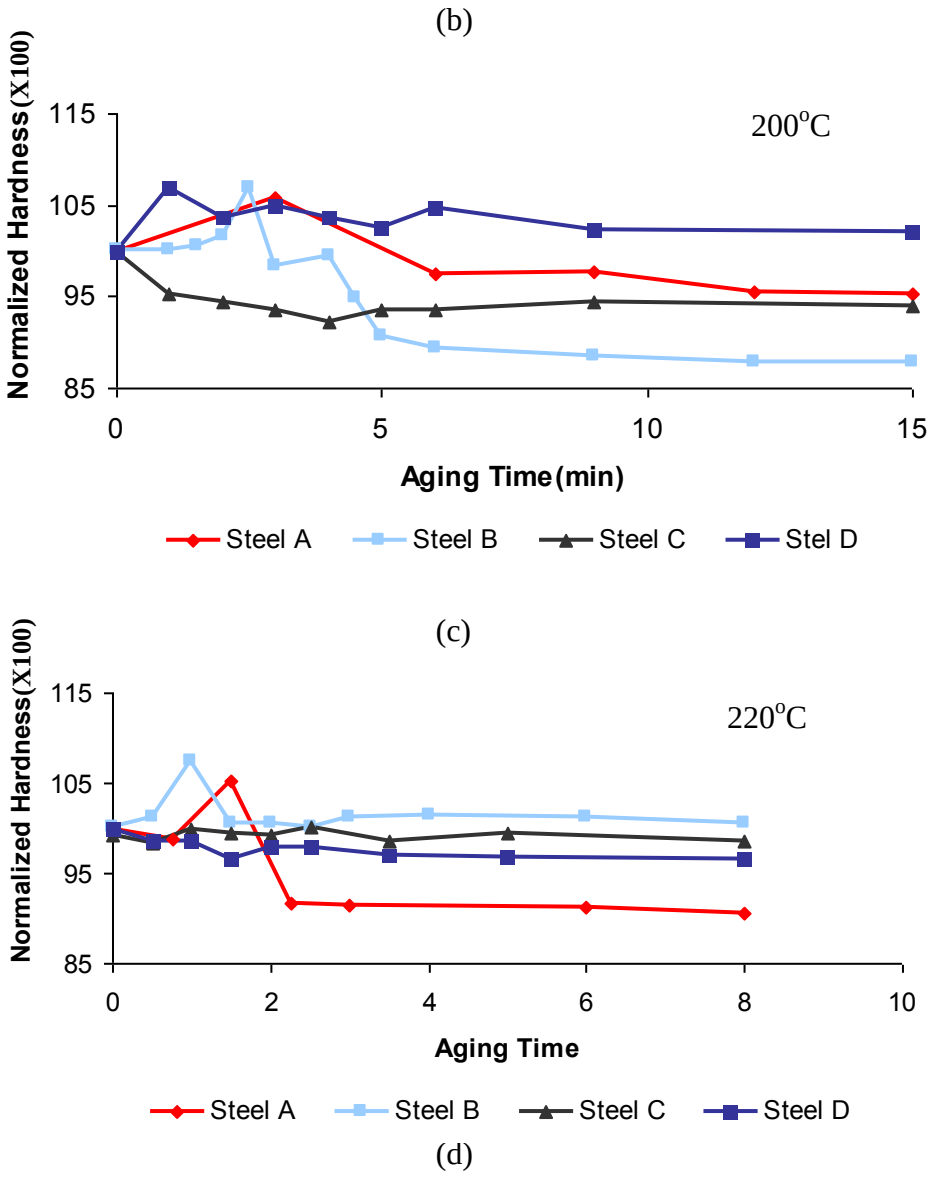


**Figure 5.3**. Normalized hardness values for different aging time at 145°C (a), 170°C (b), 200°C (c), and 220°C (d).

As seen in figure 5.2-a, hardness was sharply increased at the early stages of aging process. Time to reach maximum hardness value depended on the aging temperature. The temperature and time which yielded max hardness in Table 5.2. Aging curves indicate that high temperatures lead shorter times for max hardness. This result encouraged us to make a kinetic study by using hardness values. Aging process is essentially controlled by the diffusion of carbon and/or nitrogen to pin dislocations in the ferrite matrix.

**Table. 5.2**. Aging time correspond to the maximum hardness value on "Normalized Hardness – Aging Time" graphs

| STEEL | Time to maximum hardness value, minutes | | | |
|---|---|---|---|---|
| | 145°C | 170°C | 200°C | 220°C |
| A | 30 | 15 | 3 | 1,5 |
| B | 30 | 17,5 | 2 | 1 |
| C | 5 | 5 | -------- | --------- |
| D | 15 | 10 | 1 | --------- |

In the present study to follow the age hardening kinetics of the examined steels, Arrhenius equation;

$$1/t_r = A_r \times \exp(-Q_r / RT) \qquad \textbf{(5.1)}$$

was assumed, where $t_r$ is the time to reach max hardness , $A_r$ is a pre-exponential constant, $Q_r$ is the activation energy of strain aging, R is the gas constant [8,314 J/mol.K] and T is the absolute aging temperature. $Q_r$ values were calculated from the slope of ln (1/tr) vs. (1/T) graphs as listed in Appendix C Fig. 1-3. Table 5.3 lists the $Q_r$ values calculated from the slope of Appendix C Fig. 1-3.

The calculated activation energies for the examined three of four different steel grades were in good agreement with the activation energy of carbon or nitrogen diffusion in BCC iron during strain aging. Table 5.4 illustrates the activation energy of carbon and nitrogen diffusion in BCC iron.

As seen in figure 5.2-(a, b, c, d), hardness was sharply increased at the early stages of aging process.

**Table 5.3**. The calculated activation energies of strain aging for the examined steels

| Steel | Activation Energy of Strain Aging Q [J/mol] |
|---|---|
| A | 71415 |
| B | 77025 |
| C | Not calculated |
| D | 81467 |

**Table 5.4.** The activation energies of carbon and nitrogen diffusion in BCC iron.

| | Activation Energy Q [J/mol] |
|---|---|
| C in BCC iron | 76580 |
| N in BCC iron | 87570 |

These activation energies of strain aging obtained by hardness measurements can be correlated with the chemical compositions of the steels.

For a better understanding, some information about the formation in steels during steel making should be explained.

Figure 5.4 demonstrates the precipitation start temperature of the compounds observed in steels which the carbon content is either stabilized with titanium or with niobium. Titanium shows a high reactivity with all metalloids in the sequence oxygen, nitrogen, sulfur, carbon and phosphorus. During steel making with addition of Ti and Al, the first compounds which will be formed at high temperatures are the TiN and AlN in sequence, dependent on the level of the total sulfur, titanium and manganese content often the formation of TiS might occur. The titanium-sulfide will be transformed into a titanium carbosulfide by absorbing carbon in the austenite region. Titanium carbosulfide is a particle with the initial dissolution temperature exceeding 950°C (which is much higher than the temperature of annealing of cold-rolled steel). Therefore, the carbon bound in the carbosulfide cannot contribute to the BH effect. Microalloying with titanium alone can cause difficulties connected with the formation of carbosulfide (inevitable loss of a certain amount of carbon) [9]. TiC and NbC contribute to the BH effect by dissolution at continuous annealing line.

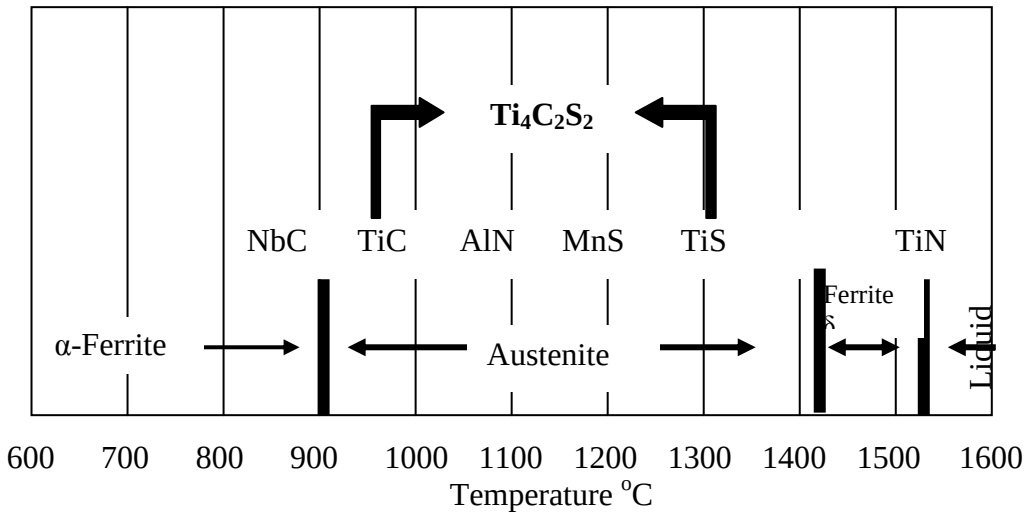


**Figure 5.4**. The precipitation start temperature of the compounds for Ti/Nb stabilized steels

To improve the strain aging, major attention has been focused on reducing the total amount of carbon and nitrogen during steelmaking and the removal of these interstitial elements from solid solution by the addition of stabilizing alloying additions, such as titanium, niobium and aluminum.

There are some equations in literature to calculate the sufficient amounts of additional elements for stabilizing.

The amount of these elements should be

$$Ti = 3.42 \times \%N + 1.5 \times \%S \quad \textbf{(5.2)}$$

$$Nb = 7.75 \times \%C \quad \textbf{(5.3)}$$

$$Al = (27/14) \times \%N \quad \textbf{(5.4)}$$

To bind the interstitial atoms (C and N)

C atom diffusion to the dislocations is the main reason of strain aging of steel A and steel B. for steel A and steel B, it is obviously clear that the content of the Ti and Al are sufficient for binding all nitrogen atoms as TiN and AlN. These compounds are formed at high temperatures and the dissolution temperatures exceeding 1000°C which is much higher than the temperature of annealing of cold-rolled steel. Therefore, the nitrogen bound in the TiN and AlN cannot contribute to the strain aging. For steel A and B, Nb content is not enough to bind the carbon atoms. At this

point, we assume that in addition to dissolution of NbC at continuous annealing temperatures, the free C atoms in the ferrite phase contributed the strain aging.

Steel D has extremely high carbon content than that of the other steels examined. On the contrary, Ti, Nb and Al contents are very limited. Ti and Al are insufficient to bind nitrogen atoms and this situation will cause to have free nitrogen in ferrite phase. It is assumed that the excess amounts of carbon atoms could bind the Fe atoms to form $Fe_3C$ (cementite) which cannot contribute the strain aging. So, this shows the calculated activation energy is in good agreement with the chemical composition of steel D.

As shown in the "Normalized Hardness – Aging Time" graphs of steel C in figure 5.3-c, there is no detectable change in the hardness values due to strain aging. Therefore it is impossible to calculate strain aging activation energy for this steel grade. It is interesting to note that, comparing to the other three steel grades steel C showed very limited strain aging.

### 5.3. Bake Hardening Behavior of the Steel

The stress – strain curves of pre-strained 2%, 5% and 10% and aged ($170^oC$) samples are illustrated in Appendix D Figure 1-4.

The Bake hardening effect was measured as the difference between the flow strength at the end of pre-straining and the lower yield strength after aging for various pre-strain and aging times at $170^oC$. Table 5.5 illustrates the BH-effect corresponding to various pre-strain ratios and aging time at $170^oC$.

In this study we compared the BH-effect by means of pre-strain and the steel grade. As can be seen in figure 5.5 maximum BH-effect was obtained at the level of 2%. However, the time needed for reaching to max. hardness values is different for steel grades. As seen in figure 5.5-b maximum hardness values was reached at the $20^{th}$ min of aging for steel A and steel B. BH-effect of steel A and steel B are related to the C atoms diffusions to the dislocations. Steel D, strain aging kinetic explained by N atoms diffusion, showed the max BH-effect at $10^{th}$ min in figure 5.5-d.

**Table 5.5.** BH-effect corresponding to various pre-strain ratios and aging time at 170°C

| Steel grade | Aging Time,min | BH-effect, MPa | | |
|---|---|---|---|---|
| | | 2% | 5% | 10% |
| A | 10 | 66 | 68 | 69 |
| | 15 | 79 | 65 | 69 |
| | 20 | 86 | 70 | 77 |
| | 30 | 66 | 69 | 68 |
| B | 10 | 66 | 19 | 77 |
| | 15 | 66 | 26 | 69 |
| | 20 | 91 | 43 | 69 |
| | 30 | 83 | 67 | 68 |
| C | 10 | 1 | 6 | 11 |
| | 15 | 1 | 8 | 51 |
| | 20 | 13 | 13 | 37 |
| | 30 | 11 | 8 | 26 |
| D | 10 | 78 | 34 | 13 |
| | 15 | 66 | 27 | 39 |
| | 20 | 61 | 25 | 37 |
| | 30 | 68 | 37 | 23 |

It should be noted that Nitrogen has a faster diffusion rate than carbon (1, 34 x $10^{16}$ $cm^2s^{-1}$ and 2.8 x $10^{17}$ $cm^2s^{-1}$, respectively) which yield aging in a relatively short time period. BH-effect values of the pre-strain level 5% and 10% were lower than that of pre-strain level 2%. The reason for this behavior could be explained by the fact that as pre-strain increases, the dislocation density increases and the amount of carbon per unit decreases. Therefore the BH-effect decreases. We could see this effect clearly in figure 5.5-a,b,d which are illustrated below.

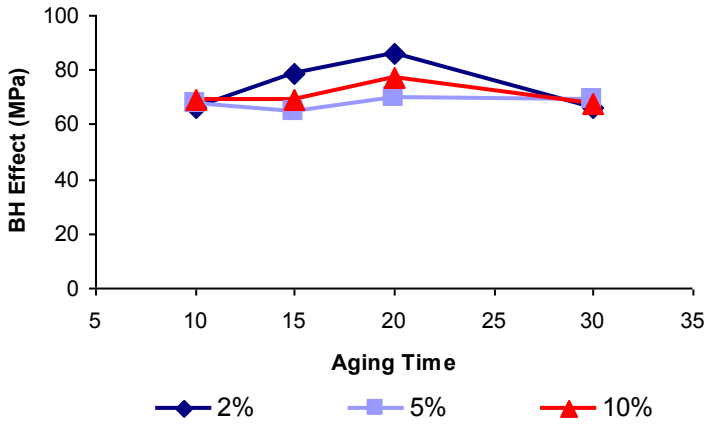


(a)

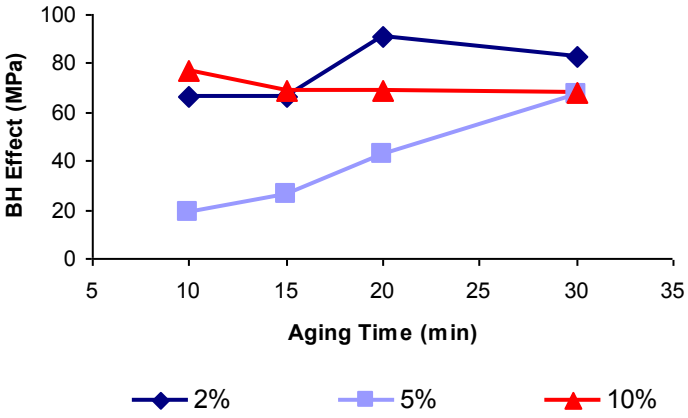


(b)

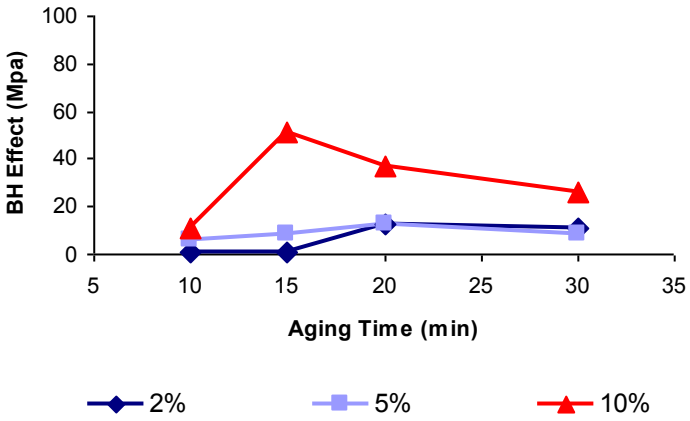


(c)

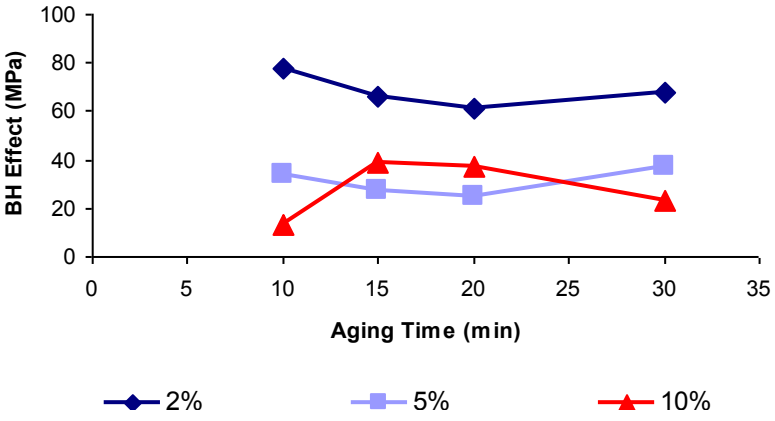


(d)

**Figure 5.5.** BH-effect of steel A (a), steel B (b), steel C (c), and steel D (d) for pre-strain level 2%,5%,10% at 170$^{o}$C

When comparing the other steel grades, effect of the pre-strain levels on 131 steel is different. As seen in figure 5.4-c the maximum ΔσBH value gained at pre-strain level of 10%.

Figure 5.6. a, b, c shows the BH-effect comparison of each steel grade for different pre-strain levels. Steel A and B show similar BH-effect. Nb content of steel A grade is not sufficient to bind all carbon atoms. We assumed that the solute carbon amounts which will affect the BH level were provided by both dissolution of NbC at continuous annealing temperatures and free C atoms existing in the ferrite phase. So the adequate level of C was provided to have a good (BH effect) bake hardenable steel. Ti and Al atoms bind all nitrogen atoms as TiN and AlN. Another important point for bake hardenable steels is the room temperature aging. The aim is to produce bake hardenable steels which have not only a good BH effect but also a good resistance to room temperature aging. As seen in the figure 5.6. a, b, c. steel B shows the best BH-effect behavior.

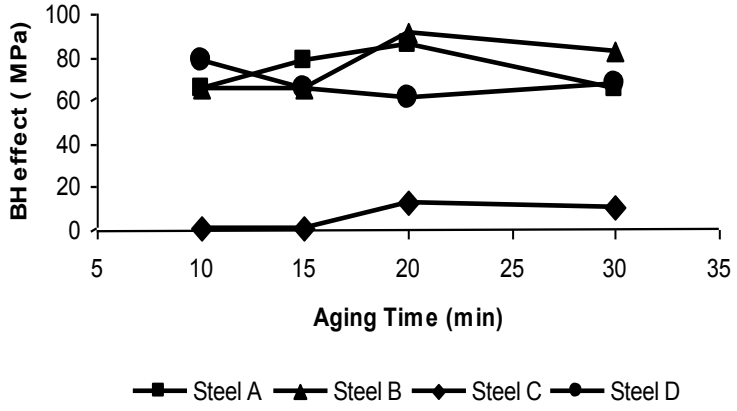


(a)

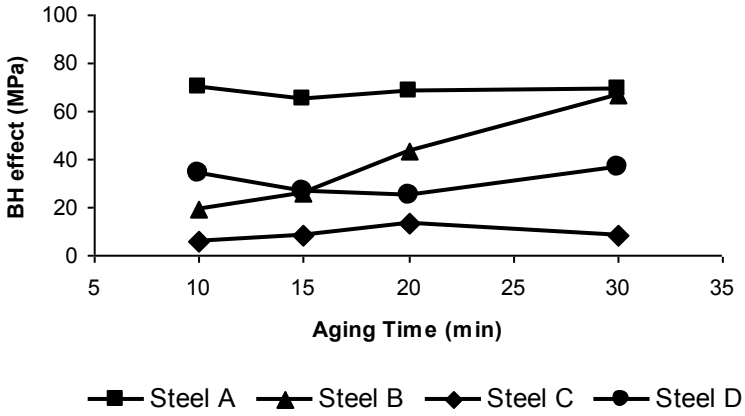


(b)

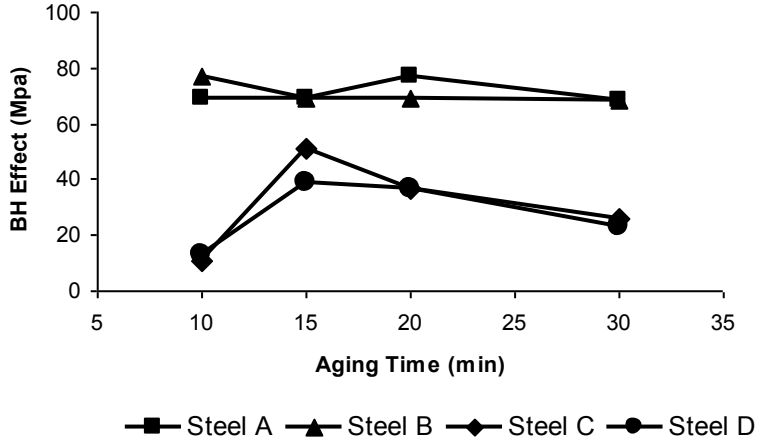


(c)

**Figure 5.6**. BH-effect of 2% pre-strain (a), 5% pre-strain for steel (b), 10% pre-strain (c) for steel A, B, C and D at 170$^{o}$C.

Steel C shows the worst BH effect. This steel grade has limited Nb content and high amount of Ti. Very limited amount of carbon were bonded to Nb. Mn content is also low comparing to the Steel grades which shows good BH effect. As mentioned before the manganese content is very important, low manganese content caused the segregation of the TiS sulfide and the titanium-sulfide will be transformed into a titanium carbosulfide by absorbing carbon in the austenite region. $Ti_4C_2S_2$ carbosulfide is insoluble under conventional annealing temperatures. C atoms that bound in the carbosulfide cannot contribute the BH effect.

## 6. CONCLUSION

Following conclusions can be drawn according to results of this study;

1. Hardness measurements performed for four different temperatures after pre-strained %2 showed that BH effect can be examined by the change in hardness values. So, it is possible to investigate the kinetics of age hardening by using hardness values
2. The calculated activation energies for the examined steel grades were in good agreement with the activation energy of carbon or nitrogen diffusion in BCC iron.
3. The maximum BH-effect was obtained at the level of 2%. Maximum hardness values was reached at the $20^{th}$ min of aging for steel A and steel B which are related to the C atoms diffusions to the dislocations and $10^{th}$ min for Steel D that the strain aging kinetic explained by N atoms diffusion.

.

## REFERENCES


[1] ***Karman Dehghani, J.J. Jonas***, May 2000. Dynamic bake hardening of IF Steels, *Metallurgical and Materials Trans*., **31A.,** 1375-1384.

[2] **L. J. Baker, S. R. Daniel, and J. D. Parker,** Apr 2002. Metallurgy and Processing of ULC Bake Hardening Steels, *Materials Science and Technology.* **Vol 18**, 355- 368.

[3] **Shimizu T., Funakawa Y., Kaneko S.,** Nov 2004, High strength steel sheets for automobile suspension and chassis use- high strength hot rolled steel sheets with excellent press formability and durability for critical safety parts, *JFE Technical Report*, **4,** 25-31.

[4] **Susumu S., Susumu O., Toshiyuki K., Osamu H., Toshitake H., Hiroshi T.,** Nov 1992. Development of bake hardening high strength cold-rolled sheet steels for automobile exposed panels, *KAWASAKI Steel Technical Report*, **27**, 31-38.

[5] ***ASM specialty Hand book,*** 1992. Carbon and alloy steels, steels for automotive applications, ASM International, Materials Park, Ohio

[6] **E. Kozeschnik, V. Pletenev, N. Zolotorevsky, and B. Buchmary**, Jun 1999. AlN precipitation and texture development in batch annealed bake hardening steel, *Metallurgical and Materials Transactions A*, **30A**, 1663-1672

[7] ***A.K. De , K. De Blauwe , S. Vandeputte , B.C. De Cooman***, 2000. Effect of dislocation density on the low temperature aging behavior of an ultra low carbon bake hardening, *Journal of Alloys and Compounds*, 405–410

[8] **Karman Dehghani, J.J. Jonas,** 2000. Dynamic bake hardening of IF Steels, *Metallurgical and Materials Trans.*, **31A,** 1375-1384.

[9] **L. M. Storozheva,** 2001. Ultralow carbon steels for the automotive industry with the effect of hardening due to drying of finished parts, *Metal Science and Heat Treatment,* **Vol. 43,** 336-344.

[10] **http://www.nkk.co.jp**

[11] **www.danchuk.com/quaterpanelpatches**

[12] **Eric Lamm,** 2001. Advanced steel solutions for Automotive lightweighting, *Windsor Workshop,* June 5, 2001

[13] **www.ussteel.com**

[14] **International Iron and steel Institute,** 2005**.** *Advanced High Strength Steel (AHSS) Application*, online at www.worldautosteel.org

[15] **http://www.krakatausteel.com/product**

[16] ***ASM specialty Hand book,*** 1992. Carbon and alloy steels, steels for automotive applications, ASM International, Materials Park, Ohio.

[17] **George E. Dieter,** 1988. *Mecanical Metallugy*, Hill Book Company, UK

[18] **ASM Metals Hand Book, 1995, volume 1,** ASM International, Materials Park, Ohio.

[19] **International Iron and steel Institute,** 2004**.** *Advanced High Strength Steel (AHSS) Application*, online at www.worldautosteel.org

[20] **Timokhina I.B., Hodgson P. D., and Pereloma E. V.,** 2004. Effect of Microstructure on the Stability of Retained Austenite in Transformation-Induced-Plasticity Steels, *Metallurgical and Materials Transactions A*, **Vol 35,** 2331- 2341.

[21] **M. Takahashi and H.K.D.H. Bhadeshia:** *Mater. Trans., JIM*, 1991,**Vol. 32**, pp. 689-96.

[22] **S. Berbenni , V. Favier , X. Lemoine , M. Berveiller,** ***2004.*** A micromechanical approach to model the bake hardening effect for low carbon steels, *Scripta Material***, 51, 303 -308**

[23] **D. K Matlock, B. J. Allan and J. G. Speers**, 1998. *Proc. Conf. on modern LC and ULC Sheet Steels for cold forming processing and properties*, Aachen Verlag, Mainz,265 – 276.

[24] **M.E. Fine, 1996.** *Metallurgical and Materials Transaction A*, **Vol 27, 2397-2418**

[25] **L. J. Baker, J. D. Parker, and S. R. Daniel,** 2002. Mechanism of bake hardening in ultralowcarbon steel containing niobium and titanium additions, *Materials Science and Technology*, **Vol 18,** 541-547

[26] **A. K. De, S. Vandeputte, and B. C. De Cooman,** 1999. *Scripta Material*, **Vol 8**, 836- 842

[27] **P. Elsen and H. P. Hougardy,** *Steel Res.*, 1993, **Vol 64**, 431- 439

[28] **W.C Leslie,** 1981. *The Physical Metaalurgy of Steels*, McGaw-Hill, NY**, 79-90**

[29] **N. Tsuchida, , E. Baba, K. Nagai, Y. Tomota,** 2005. Effects of interstitial solute atoms on the very low strain-rate deformations for an IF steel and an ultra-low carbon steel, *Acta Materialia*, **53**, 265–270

[30] **A. Van Snick, K. Lips, S. Vandeputte**, 1998. Effect of carbon content, dislocation density and carbon mobility on bake hardening, *Modern LC and ULC Sheet Steels for Cold Forming: Processing and Properties*, *Int. Symp.*, Aachen, 413 – 424

[31] **L. Storojeva, C. Escher, R. Bode, K. Hulka, 2002.** Stabilization and Processing Concept for the production of ULC steel sheet with bake hardenability, Max-Planck – institute for Iron Research

[32] **www.asminternational.org**

[33] **B. Engl and T. Gerber**, 1996 . Microalloyed, vacuum degassed high-strength steels with special emphasis on IF steels, *Steel Res.*, **67**, 430 – 437

[34] **M. Hua, C. Garcia, and A. DeArdo**, 1997. "Precipitation behavior in ultra-low-carbon steels containing titanium and niobium, *Metall. Mater. Trans.*, **28A**, 1769 – 1780

[35] **Ralph A. Mutschler, 2000.** Effect of solutes on austenite processing in ULC steels, PhD Thesis, University of Pittsburgh, USA

[36] **T. Irie, S. Satoh, A. Yasuda, and O. Hashimoto,** 1983. Development of drawable and bake-hardenable high strength steel sheet by continuous annealing of extra low-carbon steels with Nb or Ti, and P, *Metallurgy of Continuous-Annealed Sheet Steel, TMS-AIME Symposium*, Dallas, 1362 – 1369.

[37] **L. M. Storozheva, K. Éscher, R. Bode, K. Hulka, and D. A. Burko** *2002.* Effect of Nb and coilling and annealing temp. on the microstructure, mechanical properties and bake hardening of ULC steel for the automotive industry, *Metal Science and Heat Treatment* ***Vol. 44***

[38] **K. Lips, X. Yang, and K. Mols,** 1996. The effect of coiling temperature and continuous annealing on the properties of bake hardenable IF-steels, *Steel Res.,* **67**, 357 – 363

[39] **B. Soenen , A.K. De , S. Vandeputte , B.C. De Cooman,** 2004. Competition between grain boundary segregation and Cottrell atmosphere formation during static strain aging in ultra low carbon bake hardening steels, *Acta Material,* **52,** 3483–3492

## APPENDIX A

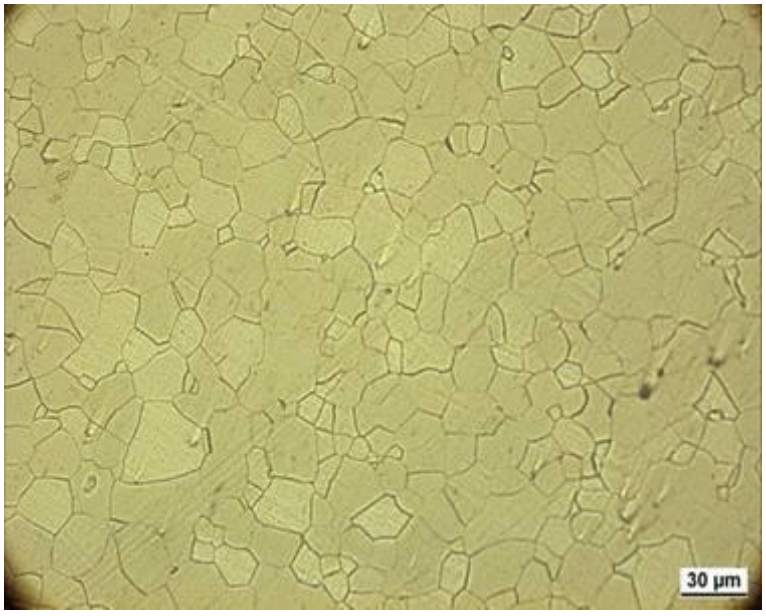


**Figure A.1**. Microstructure of Steel A, as-recieved. (X500).

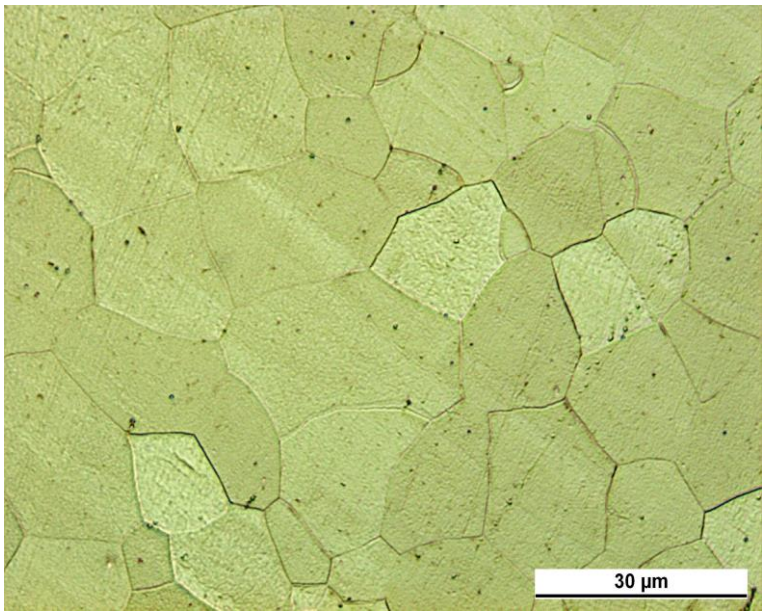


**Figure A.2**. Microstructure of Steel A, as-recieved. (X1600).

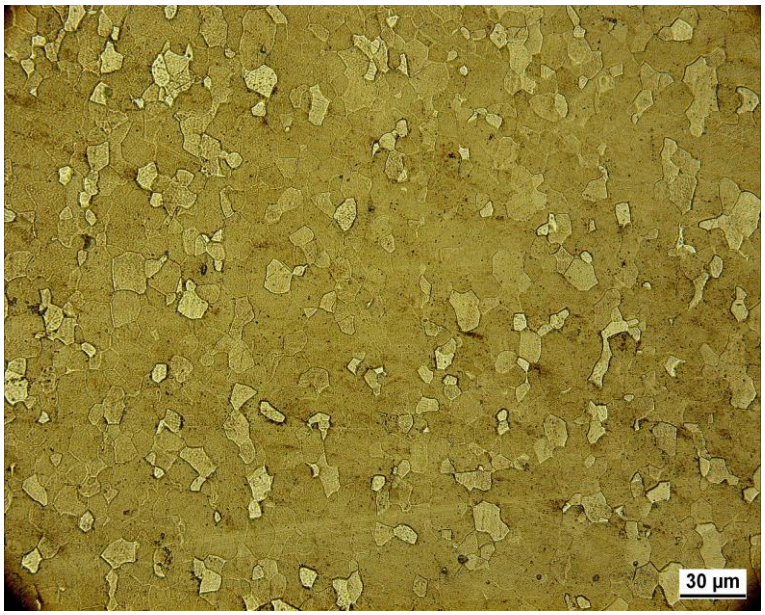


**Figure A.3**. Microstructure of Steel B, as-recieved. (X500).

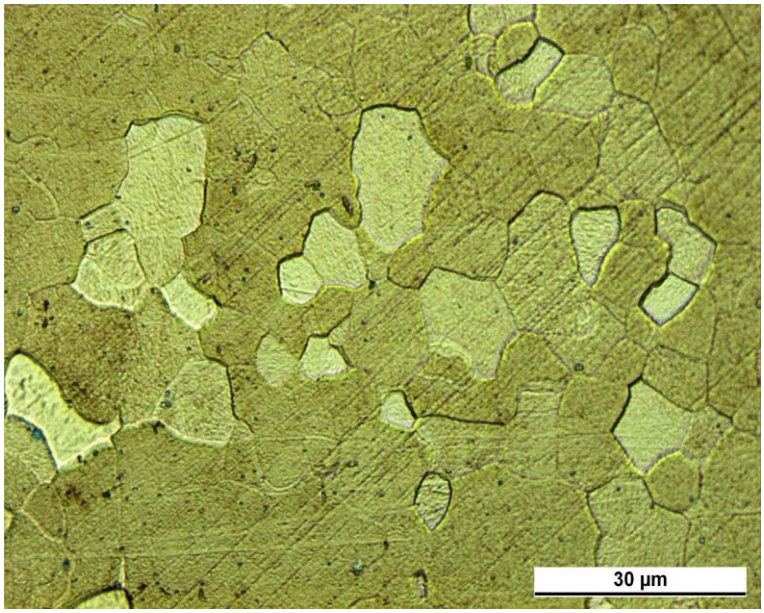


**Figure A.4.** Microstructure of Steel B, as-recieved. (X1600).


**Figure A.5.** Microstructure of Steel C, as-recieved (X500).

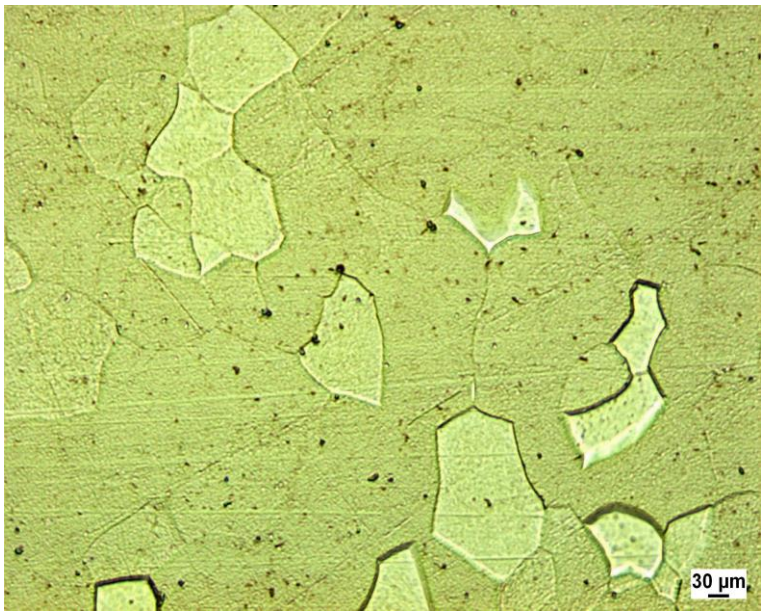


**Figure A.6.** Microstructure of Steel C, as-recieved (X1600).

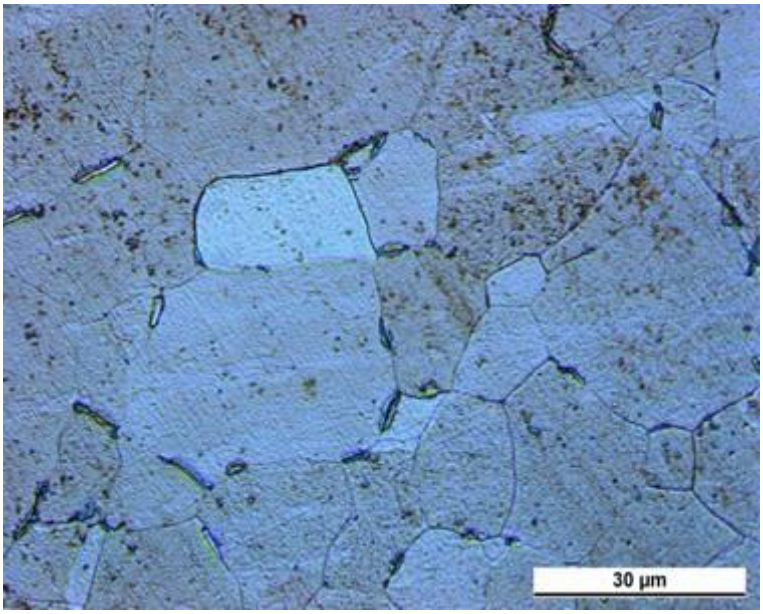


**Figure A.7.** Microstructure of Steel D, as-recieved (X1600)

## APPENDIX B

**Table B.1**. The results of hardness measurements conducted on the samples after aging for steel A.

| Time (minutes) | SAMPLE | | | | | | | |
|---|---|---|---|---|---|---|---|---|
| | STEEL A | | | | | | | |
| | 145 | | 170 | | 200 | | 220 | |
| 0 | 170.00 | ±3,2 | 170.00 | ±3,5 | 170.00 | ±2,5 | 170.00 | ±3,0 |
| 0.5 | - | | - | | - | | - | |
| 0.75 | - | | - | | - | | 167.80 | ±1,2 |
| 1 | - | | - | | - | | - | |
| 1.5 | - | | - | | - | | 179.00 | ±2,8 |
| 2 | - | | - | | - | | - | |
| 2.25 | - | | - | | - | | 155.77 | ±3,6 |
| 2.5 | - | | - | | - | | - | |
| 3 | - | | - | | 180.00 | ±3,4 | 155.30 | ±3,8 |
| 3.5 | - | | - | | - | | - | |
| 4 | - | | - | | - | | - | |
| 4.5 | | | | | | | | |
| 5 | - | | 169.00 | ±3,6 | - | | - | |
| 6 | - | | - | | 165.75 | ±2,6 | 155.00 | ±3,4 |
| 7.5 | 171.00 | ±3,2 | - | | - | | - | |
| 8 | - | | - | | - | | 154.00 | ±2,9 |
| 9 | - | | - | | 166.10 | ±3,9 | - | |
| 10 | - | | 168.00 | ±3,2 | - | | - | |
| 12 | - | | - | | 162.40 | ±3,1 | - | |
| 12.5 | - | | - | | - | | - | |
| 15 | 166.62 | ±3,02 | 180,20- | ±4,2 | 162.00 | | - | |
| 17.5 | - | | - | | - | | - | |
| 20 | - | | 180.14 | ±3,8 | - | | - | |
| 22.5 | 172.88 | ±2,26 | - | | - | | - | |
| 25 | - | | 178.12 | ±3,3 | - | | - | |
| 30 | 179.88 | ±2,6 | 176.00 | ±3,8 | - | | - | |
| 35 | - | | - | | - | | - | |
| 37.5 | 171.37 | ±3,7 | - | | - | | - | |
| 40 | - | | 171,60- | ±3,4 | - | | - | |
| 45 | 173.22 | ±2,9 | - | | - | | - | |
| 50 | 170.81 | ±3,5 | 162.40 | ±3,8 | - | | - | |
| 60 | 170.20 | ±3,1 | - | | - | | - | |
| 65 | - | | 162.00 | ±3,6 | - | | - | |
| 70 | 161.25 | ±3,8 | - | | - | | - | |
| 80 | 161.72 | ±4,03 | - | | - | | - | |

**Table B.2**. The results of hardness measurements conducted on the samples after aging for steel B

| Time (minutes) | SAMPLE | | | | | | | |
|---|---|---|---|---|---|---|---|---|
| | STEEL B | | | | | | | |
| | 145 | | 170 | | 200 | | 220 | |
| 0 | 173.00 | ±3,4 | 173.00 | ±3,07 | 173.00 | ±3,02 | 173.00 | ±2,9 |
| 0.5 | - | | - | | - | | 175.00 | ±2,4 |
| 0.75 | - | | - | | - | | - | |
| 1 | - | | - | | 173.00 | | 186.00 | ±3,2 |
| 1.5 | - | | - | | 174.00 | | 174.00 | ±2,6 |
| 2 | - | | - | | 176.00 | | 174.00 | ±3,1 |
| 2.25 | - | | - | | - | | - | |
| 2.5 | - | | - | | 185.00 | | 173.00 | ±3,4 |
| 3 | - | | - | | 170.00 | | 175.00 | ±2,9 |
| 3.5 | - | | - | | - | | - | |
| 4 | - | | - | | 172.00 | | 175.50 | ±2,3 |
| 4.5 | | | | | 164.00 | | - | |
| 5 | 171.00 | ±2,6 | - | | 157.00 | | - | |
| 6 | - | | - | | 154.50 | | 175.00 | ±3,3 |
| 7.5 | - | | 173.00 | ±3,5 | - | | - | |
| 8 | - | | - | | - | | 174.00 | ±2,6 |
| 9 | - | | - | | 153.00 | | - | |
| 10 | 172.00 | ±2,5 | 172.00 | ±3,1 | - | | - | |
| 12 | - | | - | | 152.00 | | - | |
| 12.5 | - | | 173.00 | ±2,4 | - | | - | |
| 15 | 172.00 | ±2,2 | 173.00 | ±2,5 | 152.00 | | - | |
| 17.5 | - | | 184.00 | ±3,8 | - | | - | |
| 20 | 171.00 | ±1,7 | 174.00 | ±2,4 | - | | - | |
| 22.5 | - | | 168.00 | ±2,8 | - | | - | |
| 25 | 171.00 | ±3,8 | - | | - | | - | |
| 30 | 183.00 | ±3,2 | 164.00 | ±2,3 | - | | - | |
| 35 | 168.00 | ±3,5 | - | | - | | - | |
| 37.5 | - | | - | | - | | - | |
| 40 | 169.00 | ±2,6 | 165.00 | ±2,9 | - | | - | |
| 45 | - | | - | | - | | - | |
| 50 | 159.00 | ±4,2 | 160.00 | ±3,1 | - | | - | |
| 60 | 159.00 | ±3,8 | - | | - | | - | |
| 65 | - | | 160.00 | ±3,4 | - | | - | |
| 70 | 159.00 | ±3,6 | - | | - | | - | |
| 80 | 159.00 | ±3,3 | - | | - | | - | |

**Table B.3**. The results of hardness measurements conducted on the samples after aging for steel C.

| Time (minutes) | SAMPLE | | | | | | | |
|---|---|---|---|---|---|---|---|---|
| | STEEL C | | | | | | | |
| | 145 | | 170 | | 200 | | 220 | |
| 0 | 125.00 | ±1,1 | 125.00 | ±2,05 | 125.00 | ±1,5 | 125.00 | ±3,02 |
| 0.5 | - | | - | | - | | 123.00 | |
| 0.75 | - | | - | | - | | | |
| 1 | - | | - | | 119.00 | ±2,3 | 123.55 | ±2,1 |
| 1.5 | - | | - | | - | | 123.00 | ±1,9 |
| 2 | - | | - | | 118.00 | ±2,5 | 122.50 | ±1,5 |
| 2.25 | - | | - | | - | | | |
| 2.5 | - | | - | | - | | 123.6 | |
| 3 | - | | - | | 117.00 | ±1,9 | 121.9 | ±1,8 |
| 3.5 | - | | - | | - | | | |
| 4 | - | | - | | 115.37 | ±2,4 | | |
| 4.5 | - | | - | | - | | | |
| 5 | 128.00 | ±1,5 | 128.28 | ±2,3 | 116.87 | ±1,5 | 123.00 | ±1,5 |
| 6 | - | | - | | 116.87 | ±2,2 | | |
| 7.5 | - | | - | | - | | | |
| 8 | - | | - | | - | | 121.8 | ±1,3 |
| 9 | - | | - | | 118.00 | ±2,1 | | |
| 10 | 127.81 | ±2,6 | 125.25 | ±1,9 | - | | | |
| 12 | - | | - | | - | | | |
| 12.5 | - | | - | | - | | | |
| 15 | 127.00 | ±1,8 | 123.77 | ±1,8 | 117.50 | ±2,4 | | |
| 17.5 | - | | - | | - | | | |
| 20 | 124.50 | ±1,8 | 121.87 | ±1,6 | - | | | |
| 22.5 | - | | - | | - | | | |
| 25 | 123.90 | ±2,0 | 122.11 | ±1,7 | - | | | |
| 30 | 123.08 | ±1,2 | 121.10 | ±1,5 | - | | | |
| 35 | 125.11 | ±2,2 | 119.44 | ±1,7 | - | | | |
| 37.5 | - | | - | | - | | | |
| 40 | 124.88 | ±2,1 | 118.25 | ±2,1 | - | | | |
| 45 | - | | - | | - | | | |
| 50 | 124.75 | ±1,9 | 117.71 | ±1,3 | - | | | |
| 60 | 124.42 | ±1,8 | - | | - | | | |
| 65 | - | | 117.77 | ±1,8 | - | | | |
| 70 | 119.00 | | - | | - | | | |
| 80 | 118.00 | | - | | - | | | |

**Table B.4**. The results of hardness measurements conducted on the samples after aging for steel D

| Time (minutes) | SAMPLE | | | | | | | |
|---|---|---|---|---|---|---|---|---|
| | STEEL D | | | | | | | |
| | 145 | | 170 | | 200 | | 220 | |
| 0 | 143.00 | ±3,02 | 143.00 | ±3,7 | 143.00 | ±2,1 | 143.00 | ±2,8 |
| 0.5 | - | | - | | - | | 146.8 | ±2,5 |
| 0.75 | - | | - | | - | | | |
| 1 | - | | - | | 153.00 | ±2,8 | 146.9 | ±2,1 |
| 1.5 | - | | - | | - | | 144 | ±2,5 |
| 2 | - | | - | | 148.25 | ±2,7 | 145.8 | ±2,4 |
| 2.25 | - | | - | | - | | | |
| 2.5 | - | | - | | - | | 146 | ±1,3 |
| 3 | - | | - | | 150.00 | ±3,1 | | |
| 3.5 | - | | - | | - | | 144.6 | ±2,7 |
| 4 | - | | - | | 148.22 | ±2,9 | | |
| 4.5 | - | | - | | - | | | |
| 5 | 144.00 | ±3,7 | 150.00 | ±3,5 | 146.60 | ±2,5 | 144 | ±2,3 |
| 6 | - | | - | | 149.75 | ±2,8 | | |
| 7.5 | - | | - | | - | | | |
| 8 | - | | - | | - | | 143.8 | ±2,0 |
| 9 | - | | - | | 146.33 | ±2,9 | | |
| 10 | 144.70 | ±2,7 | 162.00 | ±1,6 | - | | | |
| 12 | - | | - | | - | | | |
| 12.5 | - | | - | | - | | | |
| 15 | 153.77 | ±1,9 | 165.00 | ±1,9 | 146.10 | | | |
| 17.5 | - | | - | | - | | | |
| 20 | 150.09 | ±2,5 | 150.00 | ±2,5 | - | | | |
| 22.5 | - | | - | | - | | | |
| 25 | 145.91 | ±1,6 | 150.00 | ±2,1 | - | | | |
| 30 | 144.88 | ±1,9 | 148.00 | ±2,0 | - | | | |
| 35 | 143.00 | ±2,0 | 146.00 | ±2,5 | - | | | |
| 37.5 | - | | - | | - | | | |
| 40 | 146.38 | ±1,6 | 147.00 | ±1,5 | - | | | |
| 45 | - | | - | | - | | | |
| 50 | 144.90 | ±1,7 | 148.00 | ±2,3 | - | | | |
| 60 | 144.13 | ±1,8 | - | | - | | | |
| 65 | - | | 146.00 | ±1,9 | - | | | |
| 70 | 140.00 | ±1,9 | - | | - | | | |
| 80 | 140.00 | ±2,5 | - | | - | | | |

## APPENDIX C

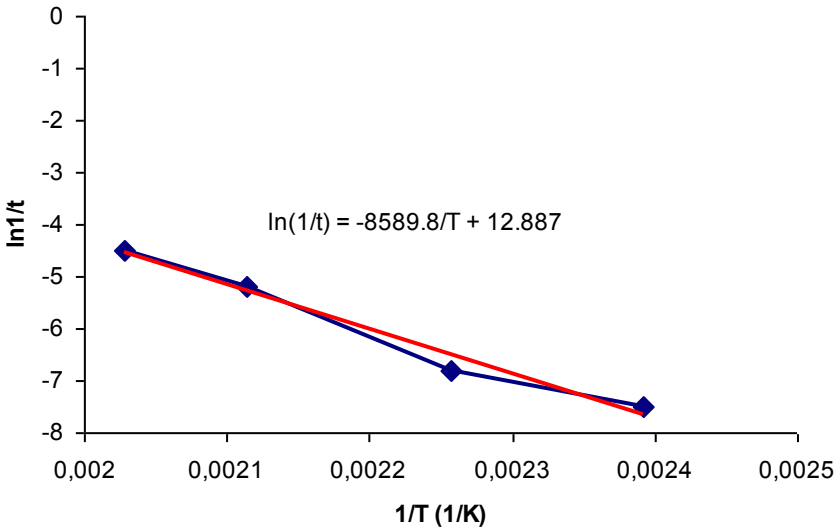


**Figure C.1.** ln (1/tr) vs. (1/T) graphs for steel A

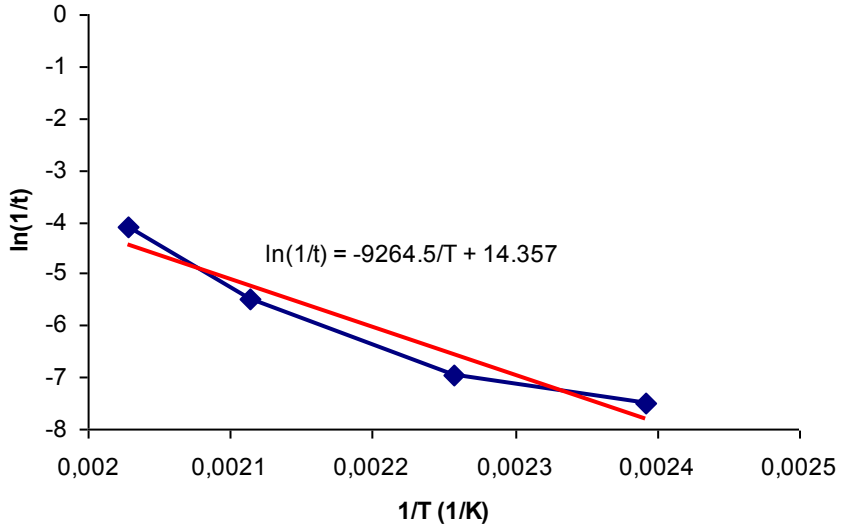


**Figure C.2.** ln (1/tr) vs. (1/T) graphs for steel B

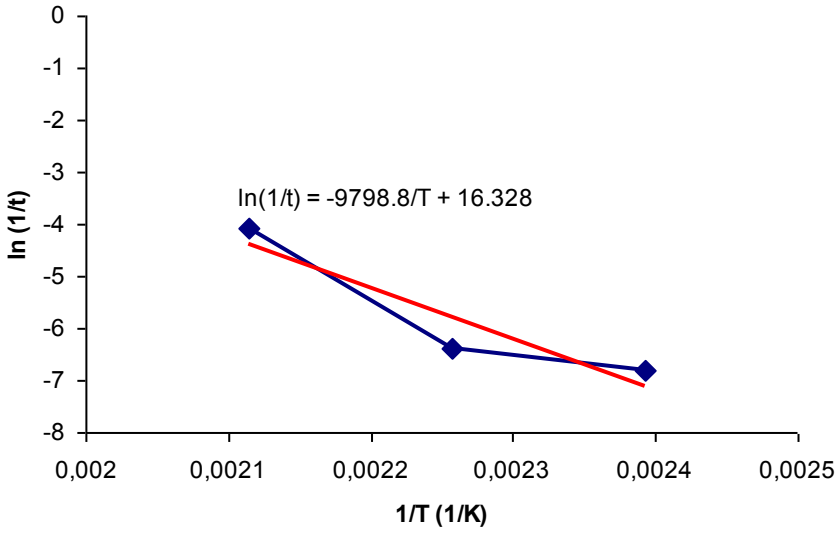


**Figure C.3**. ln (1/tr) vs. (1/T) graphs for steel D.

## APPENDIX D

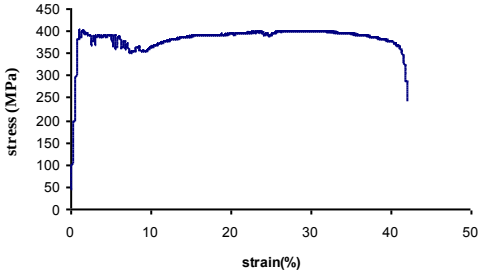


a)

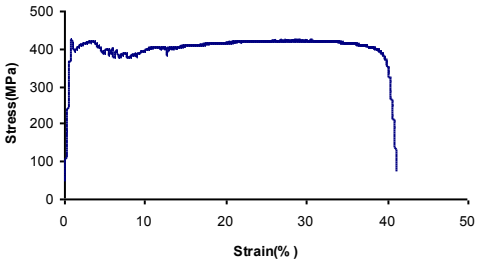


b)

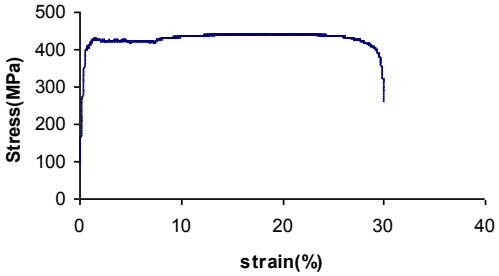


c)

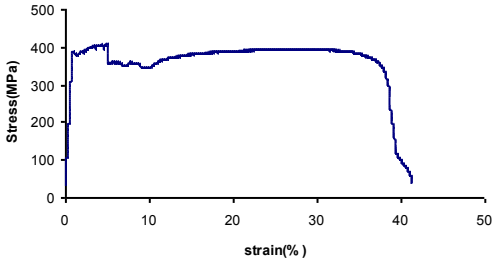


d)

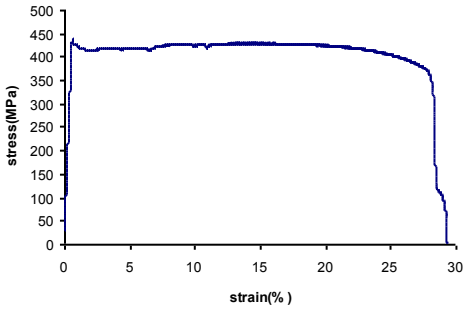


e)

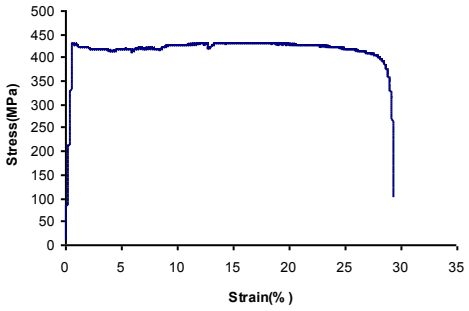


f)

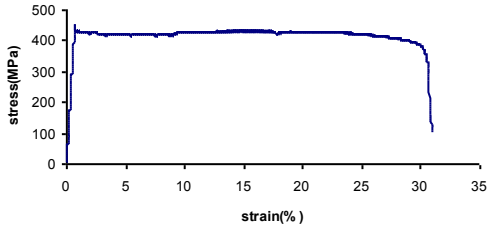


g)

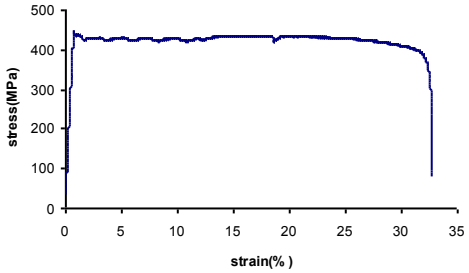


h)

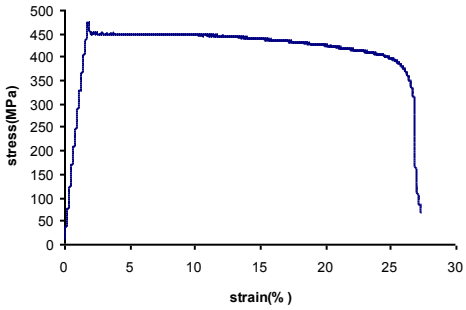


i)

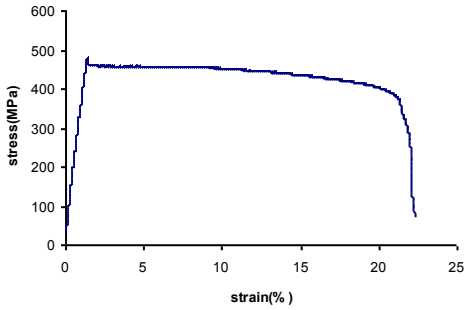


j)

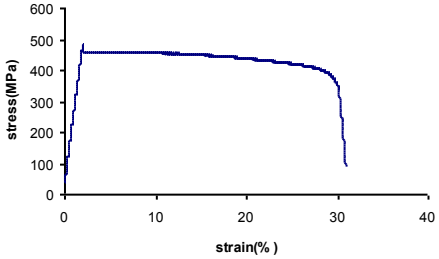


k)

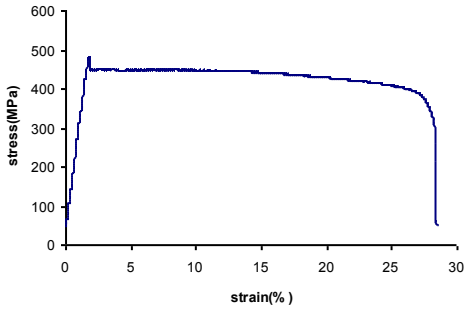


l)

**Figure D.1**. Stres-Strain curve of 2%, 5% and 10% predeformed Steel A at 10, 15, 20, 30 minute aged sample, a) 2% predeformed-10min. aged, b)2% predeformed 15min. aged, c)2% predeformed 20min. aged, d)2%predeformed 30min. aged, e) 5% predeformed 10min. aged, f)5% predeformed 15min. aged, g)5% predeformed 20min. aged, h)5%predeformed 30min. aged, i) 10% predeformed 10min. aged, j)10% predeformed 15min. aged, k)10% predeformed 20min. aged, l)10%predeformed30min.aged.

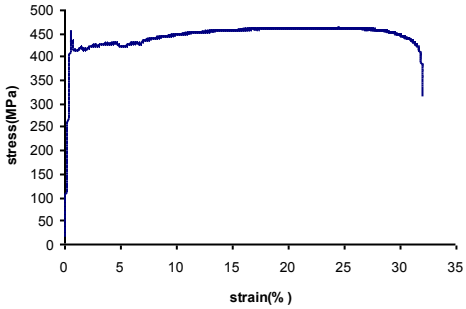
stress(MPa)
strain(% )

a)

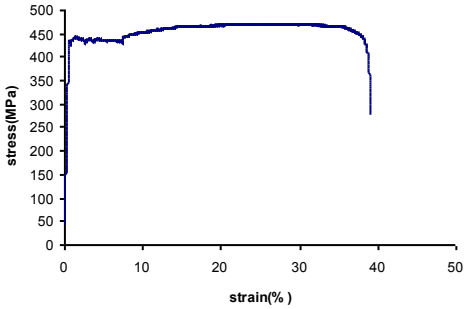
stress(MPa)
strain(% )

b)

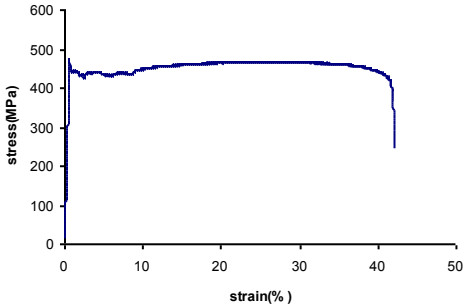
stress(MPa)
strain(% )

c)

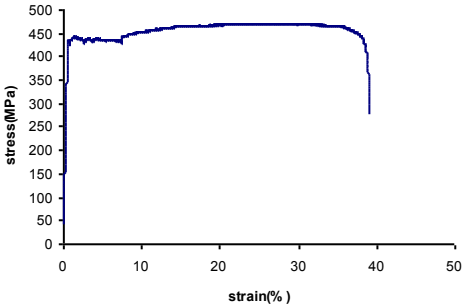
stress(MPa)
strain(% )

d)

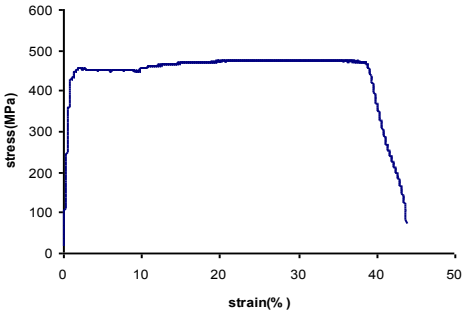
stress(MPa)
strain(% )

e)

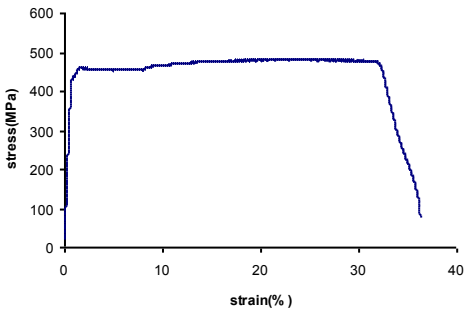
stress(MPa)
strain(% )

f)

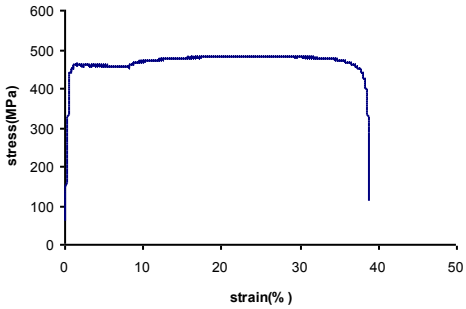
stress(MPa)
strain(% )

g)

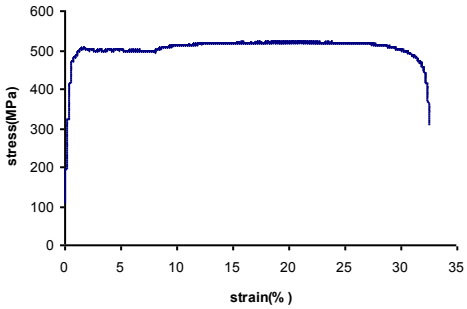
stress(MPa)
strain(% )

h)

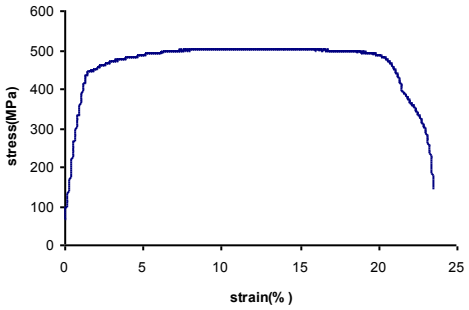


i)

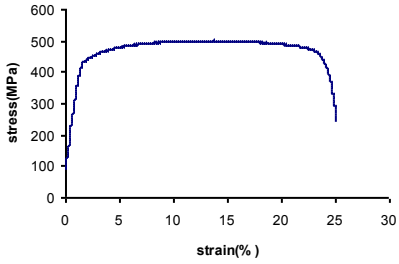


j)

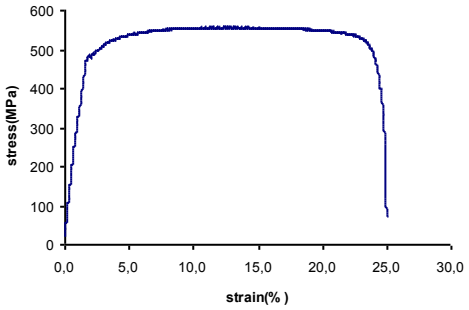


k)

**Figure D.2**. Stres-Strain curve of 2%, 5% and 10% predeformed Steel B at 10, 15, 20, 30 minute aged sample, a) 2% predeformed-10min. aged, b)2% predeformed 15min. aged, c)2% predeformed 20min. aged, d)2%predeformed 30min. aged, e) 5% predeformed 10min. aged, f)5% predeformed 15min. aged, g)5% predeformed 20min. aged, h)5%predeformed 30min. aged, i)10% predeformed 10min. aged, j)10% predeformed 15min. aged, k)10% predeformed 20min. aged,

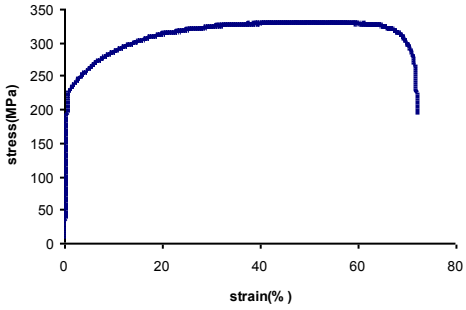
stress(MPa)
strain(% )

a)

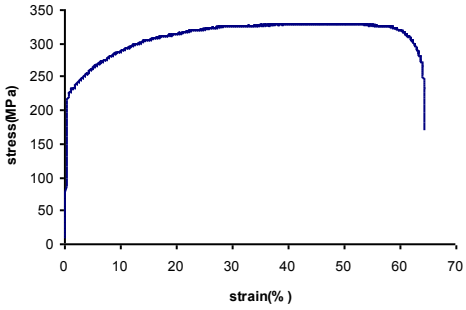
stress(MPa)
strain(% )

b)

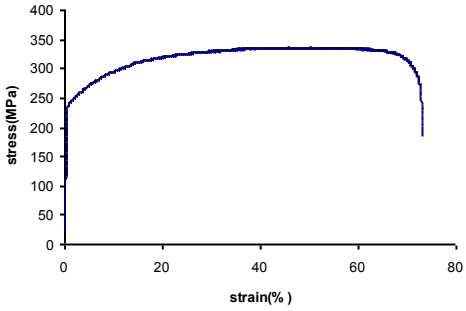
stress(MPa)
strain(% )

c)

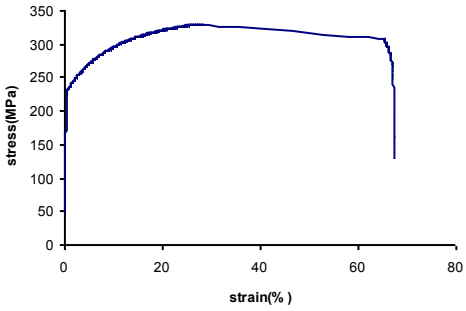
stress(MPa)
strain(% )

d)

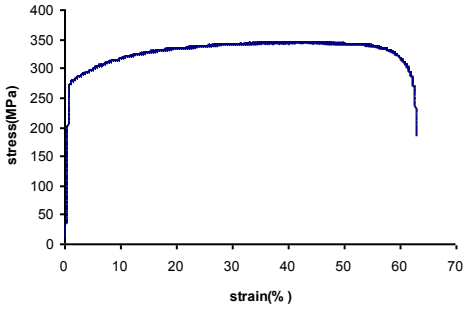
stress(MPa)
strain(% )

e)

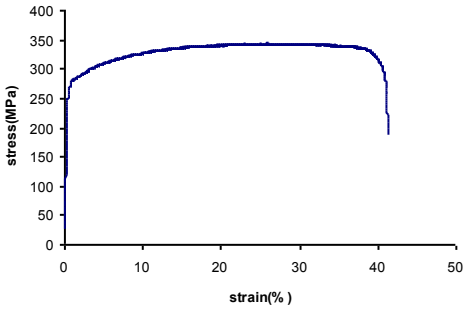
stress(MPa)
strain(% )

f)

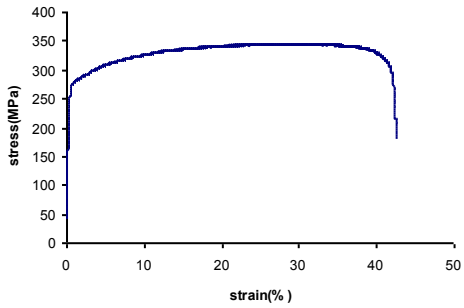


g)

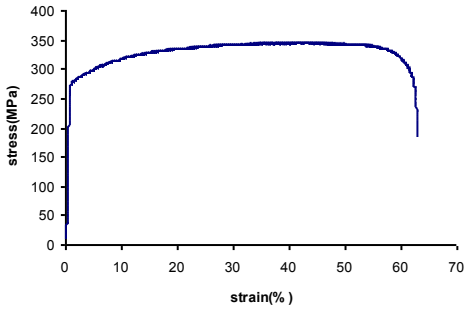


h)

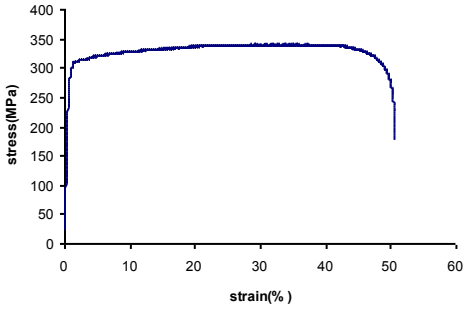


i)

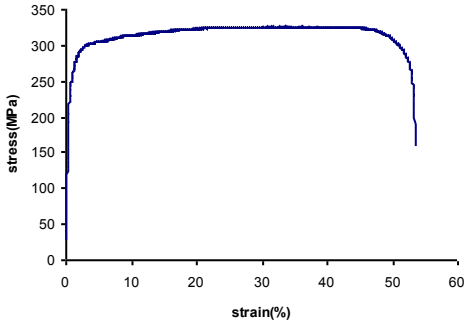


j)

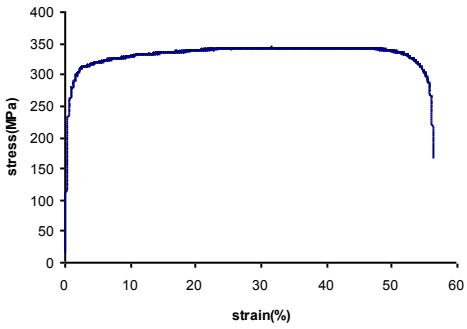


k)

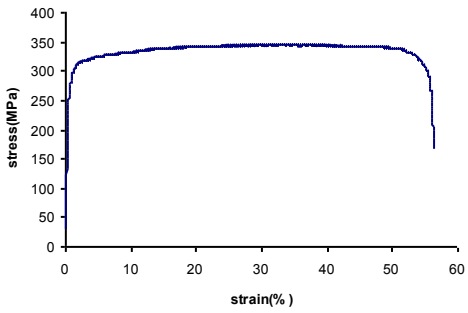


l)

**Figure D.3**. Stres-Strain curve of 2%, 5% and 10% predeformed Steel C at 10, 15, 20, 30 minute aged sample, a) 2% predeformed-10min. aged, b)2% predeformed 15min. aged, c)2% predeformed 20min. aged, d)2%predeformed 30min. aged, e) 5% predeformed 10min. aged, f)5% predeformed 15min. aged, g)5% predeformed 20min. aged, h)5%predeformed 30min. aged, i)10% predeformed 10min. aged, j)10% predeformed 15min. aged, k)10% predeformed 20min. aged, l)10%predeformed30min.aged.

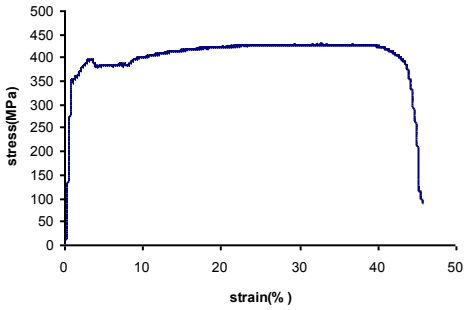
stress(MPa)
strain(% )

a)

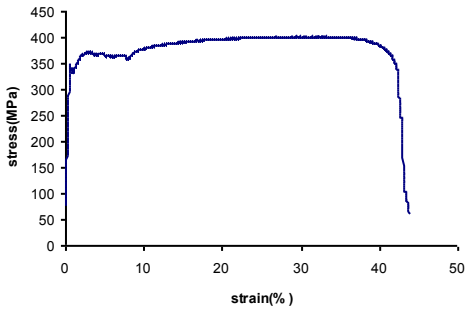
stress(MPa)
strain(% )

b)

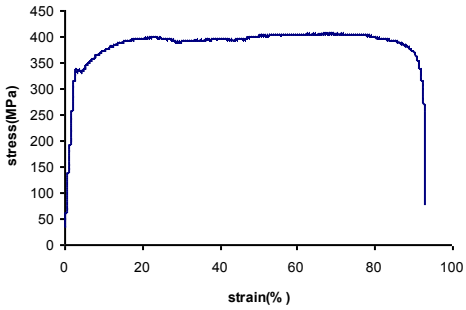
stress(MPa)
strain(% )

c)

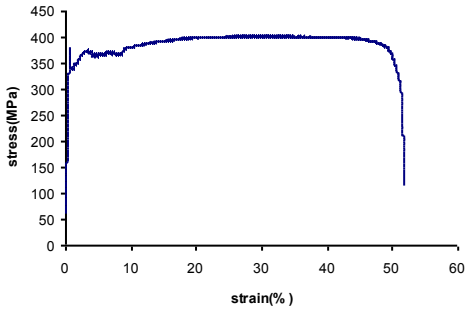
stress(MPa)
strain(% )

d)

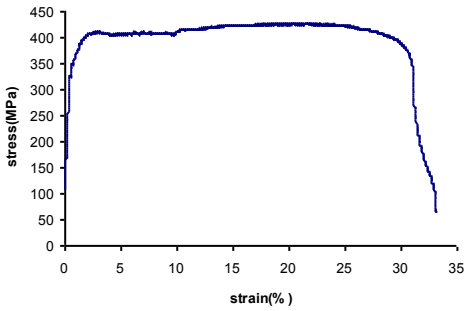
stress(MPa)
strain(% )

e)

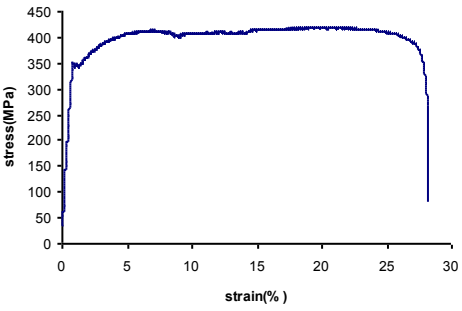
stress(MPa)
strain(% )

f)

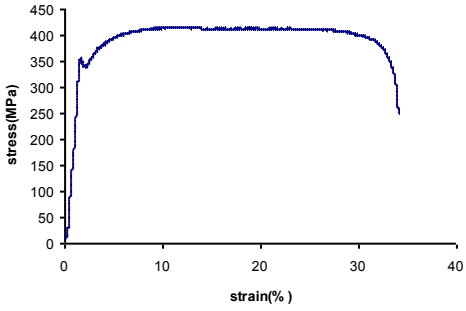
stress(MPa)
strain(% )

g)

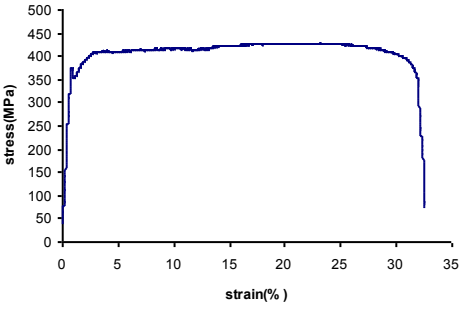
stress(MPa)
strain(% )

h)

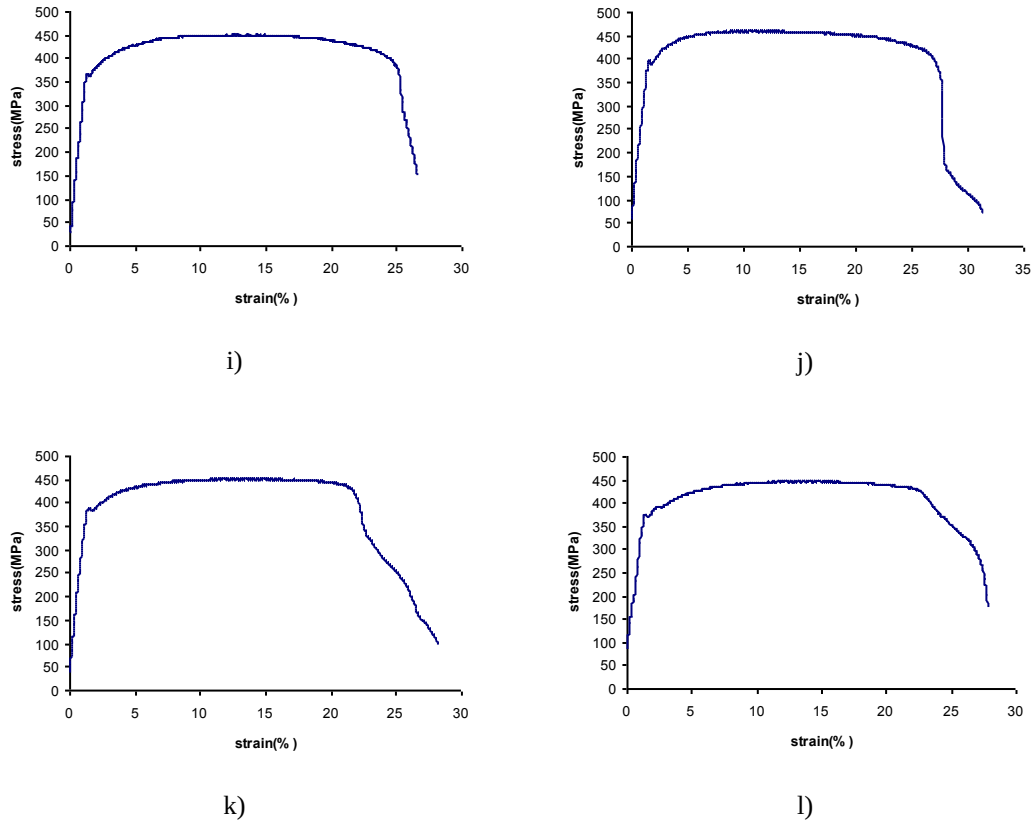


**Figure D.4**. Stres-Strain curve of 2%, 5% and 10% predeformed Steel D at 10, 15, 20, 30 minute aged sample, a) 2% predeformed-10min. aged, b)2% predeformed 15min. aged, c)2% predeformed 20min. aged, d)2%predeformed 30min. aged, e) 5% predeformed 10min. aged, f)5% predeformed 15min. aged, g)5% predeformed 20min. aged, h)5%predeformed 30min. aged, i)10% predeformed 10min. aged, j)10% predeformed 15min. aged, k)10% predeformed 20min. aged, l)10%predeformed30min.aged.

## BIOGRAPHY

Seval Türkoğlu was born in Van, Turkey in 1979. She graduated from the Haydarpaşa High School in 1997 and entered Metallurgical and Materials Engineering Department of Istanbul University in 1998. She was honoured the degree of B.Sc. in 2002. She started her graduate study at the Institute of Science and Technology in the Materials Science and Engineering Programme at the Istanbul Technical University.